Chapter IV

Phenomenological Study of Two-Body Nuclear Molecular Configurations in the Highly Excited Energy Region

Yasuhisa ABE, Yosio KONDŌ* and Takehiro MATSUSE**

Research Institute for Fundamental Physics, Kyoto University, Kyoto 606
and Centre de Recherches Nucléaires, 67037 Strasbourg
**Nuclear Physics Laboratory, University of Pittsburgh*
Pittsburgh, Pa. 15260
***Department of Physics, University of Tokyo, Tokyo 113*

(Received December 24, 1979)

Contents

§ 1. Introduction

In the preceding chapters it was shown that the molecular viewpoints are very successful in explaining the structure of the low excited states of light nuclei. Not only $4n$ self-conjugate nuclei but also other nuclei are shown to have a number of states with well-developed cluster or molecular structures. It is natural to expect that the study based on such viewpoints could be fruitfully extended to the highly excited energy region and to heavier systems as pointed out by Ikeda, Takigawa and Horiuchi[1a] more than ten years ago. Further qualitative study of the molecular structure in the highly excited energy region has been presented by Horiuchi, Ikeda and Suzuki in the Supplement No. 52 of the Progress of Theoretical Physics.[1b] From the consideration of the threshold energy rule and the characteristic features of the interaction between composite nuclei,[1c] nuclear molecular configurations in heavier systems should be expected in the systems ^{12}C-^{12}C, ^{12}C-^{16}O and ^{16}O-^{16}O at higher excitation energies. It is also believed that nuclear molecular states could be observed as resonances in heavy-ion scattering and reactions.

Since Almqvist, Bromley and Kuehner[2] have discovered the resonances in the ^{12}C-^{12}C reaction near and below the Coulomb barrier, many experimental data on the resonance phenomena in light heavy-ion reactions have been accumulated. For the experimental data[3] and theoretical discussions[4] the reader is referred to several excellent review articles. In the experimental data there is evidence for many resonance-like phenomena. We have not, however, been able to find information about the reaction mechanism and nuclear structure which is as clear-cut as, for example, the single particle resonances which emerge from the study of the α-cluster structure in low-lying states.

In order to interprete the sub-Coulomb resonances in the ^{12}C-^{12}C system, Nogami[5] has proposed the picture of nuclear molecules where two nuclei form quasi-stationary states by falling temporarily into a bound or quasi-bound state in a potential well due to the loss of the relative kinetic energy by an excitation of the collective states of nuclei. Consideration of resonance phenomena in heavy-ion reactions from the phenomenological point of view began from here. Imanishi[6] has formulated the picture in the coupled-channel framework and applied the method to the three prominent resonances first observed in the ^{12}C-^{12}C system. He could reproduce many features of the resonances fairly well, but the result was criticized seriously.[7] The points of the criticism are i) the use of a weak absorptive potential ($W\approx 100$ keV) which might be inconsistent with the total reaction cross section, ii) a too small number of resonances predicted, compared with that observed in later experiments, and iii) the arbitrary change of the potential depth in the inelastic channel. The present authors[8] succeeded in reproducing both the average yield of the total reaction cross section and a sufficient number of narrow resonances by extending the model space up to the mutual excitation of the two carbon nuclei to

their collective 2^+ (4.44 MeV) state. This overcame the problems presented by points i) and ii). Recently many resonances have been observed at energies above the Coulomb barrier as well. Experimental and theoretical attempts are being made in order to clarify the phenomena.[3),4)]

In order to explain the intermediate structure observed in the elastic excitation function of the $^{16}O+^{16}O$ system at energies well above the Coulomb barrier, Scheid, Greiner and Lemmer[9)] have applied the Nogami-Imanishi model with particular emphasis on a double resonance mechanism, where first an elastic partial wave resonates with its corresponding virtual state and then a quasi-bound or bound state in an inelastic channel is excited by this wave. Although all of the above efforts based on the molecular picture succeeded to some extent in reproducing the resonant phenomena and although the picture seems to be quite simple and promising, it had not been commonly accepted. At this time the existence of molecular configurations had not yet been established in the highly excited energy region of ligh nuclei. One of the reasons could be that no one had given a general systematic prediction for the occurrence and fading-away of resonances by a simple argument based on this picture.

The theoretical and experimental situations indicate that the study of the nuclear molecular structure in the highly excited energy region differs essentially from that in low-lying states of light nuclei. As has been mentioned in Chapter I, many degrees of freedom become active in the highly excited energy region and accordingly the level density of the compound state is very high as has been well known since Bohr's compound nucleus hypothesis. Another point is that many reaction channels are open in the energy region. Therefore it is natural to expect that simple states such as single particle resonances might be dispersed by the coupling with many complex states of the compound nucleus and then they are able to decay through many open channels. Later we will discuss these points more carefully for grazing partial waves.

From the above naive considerations, it is evident that the study of nuclear molecular states in the highly excited energy region is more difficult and complex than the study of those in the low excited energy region. In other words, in order to make progress in the study of nuclear molecular structures in the energy region, we have to study not only the individual character of the structures, but also the bulk properties of the heavy ion reaction mechanism. This means that we should be careful in setting up an imaginary part of the optical potential, by which we usually describe other degrees of freedom than those taken into account explicitly.

On the imaginary part of the interaction potential between heavy ions, almost nothing has been clarified theoretically. Even the concept of optical potential has not yet been justified, which is completely different from the

case of nucleon and light particle reactions. However, one characteristic aspect of the optical potential, i.e., "surface transparency" has been demonstrated for several combinations of light heavy ions.[10] The character of the surface transparency of the interaction potential may be related to properties of the compound nucleus and of direct reaction channels. At energies well above the Coulomb barrier the heavy-ion incident flux brings in rather large angular momenta. The partial waves with such large angular momenta might then neither be accomodated by the compound states of composite system because of the low level density of the states with the corresponding spins, nor have well-matched reaction channels into which the flux can flow except for collective inelastic channels. This is actually the case for systems such as ^{12}C-^{12}C, ^{12}C-^{16}O and ^{16}O-^{16}O. In these systems the incident channels have symmetric or nearly symmetric mass partitions and the reaction Q-values are small. The weak absorption in grazing partial waves will be discussed in the light of the recent phenomenological study of the fusion cross section in light heavy-ion reactions.[11a)]

It is presumably meaningful to discuss single-particle resonances in a real nuclear potential for systems which have the weak absorption region mentioned above. The essential character of single particle states obtained in the microscopic study of interactions between composite nuclei is, as will be given in Chapter V, that there exist bound or quasi-bound states in the relative motion between composite nuclei such as ^{16}O-^{16}O[12] and ^{12}C-^{16}O,[13] and that the energies of these states are in rotational sequence. The corresponding wave functions of the relative motion are well localized at the surface region. It is also well known that the phenomenological potential with a soft core at the inner region, which is expected as the effect of the Pauli exclusion principle between composite nuclei, can roughly reproduce the series of bound or quasi-bound states with the rotational energy sequence. Thus the existence of a potential-resonance band (the elastic molecular-rotational band) is considered to be one of the general features in the interaction between heavy-ions.

From the viewpoint of nuclear molecules, the present authors[14] have proposed a Band Crossing Model (BCM) in order to understand a possible resonance mechanism of the two-body nuclear molecular motion. The existence of the elastic molecular-rotational band mentioned above makes it possible to discuss systematically at what spin values Nogami's picture will be valid with a specific excited molecular configuration as a dominant component. When the projectile or the target is excited to a collective state with the intrinsic spin I and the excitation energy ΔE (equal to the Q-value of the inelastic channel considered), we have several quasi-rotational bands in the inelastic channel according to the angular momentum coupling between the intrinsic spin I and the orbital angular momentum L. (The total angular momentum $J=|L-I|$, $\cdots$, $L+I$. We have assumed that both projectile and target nuclei have spin

zero in their ground states.) All of them, however, do not always appear as prominent resonances, because they do not necessarily carry large amounts of a partial width of the incident channel. A notable observation is that one of these bands in which the total angular momentum J is the sum $I+L$ and which has therefore been designated as the "aligned" rotational band crosses the elastic molecular-rotational band. Around the crossing point the resonance energies of the members of the elastic and of the inelastic molecular bands are very close to each other. In this region the situation just corresponds to a perturbation of the nearly degenerate system if a coupling interaction between two channels is switched on. As a result of the interaction we will have two resonances which have approximately half of the single particle widths of the elastic and the inelastic potential resonances. Not only the crossing point but also the region where the strong mixing is expected between two molecular bands can be simply discussed by the use of the moment of inertia of the elastic molecular band, and the intrinsic spin and the excitation energy of the collective state of the target and/or the projectile. We can thus obtain an overview of the occurrence of the two-body nuclear molecular resonances. In this chapter we will investigate the two-body nuclear molecular configurations, especially ^{12}C-^{12}C, ^{12}C-^{16}O and ^{16}O-^{16}O configurations, at the energy region well above the Coulomb barrier by the use of the BCM. It is worth noticing here that band crossing region just overlaps with the "surface transparent" region of the interaction potential as mentioned above for those systems.

Many excellent experimental data have recently appeared on the three systems mentioned above.[15)~17)] Angle-integrated excitation functions have been measured for the inelastic sacttering to the collective rotational or to the vibrational excited states of the projectile or the target nucleus. They have clearly shown the existence of a series of resonance-like anomalies in each system which seem to form a quasi-rotational band, although precise spin assignment has not yet been made for these resonances. Their spins, however, can be conjectured from spin assignments in other reaction channels and from the analysis of the observed fusion cross section, which will be discussed in a later section.

It is worth remarking here that the angle-integrated data are extremely valuable, because an anomaly observed there no longer comes from an interference between amplitudes with different spin values. Another important aspects of the anomalies are that they are observed to be correlated among several reaction channels, although not among all the possible decay channels. This suggests that the anomalies are not due to fluctuations of compound nucleus states, but due to resonances. In this chapter we will be mainly concerned with such experimental data.

Recently several authors[18)] have pointed out a possibility that the anomalies could be explained by the matching of angular momentum windows (L-

windows) between the elastic and the inelastic channels. They are nothing but the analogue of the effective barrier crossing in the BCM. The L-windows are, however, expected to be wider than the typical widths observed. Actually the energy range covered by resonances which are discovered to have the same spin indicates that the widths of L-windows of the active partial waves are several MeV wide. Another basic assumption of the approach is strong absorption, which seems to be inconsistent with large yields observed in the inelastic channel. For example, the peak at about $E_{\text{c.m.}}=24.5$ MeV in the 2_1^+ (4.44 MeV) inelastic excitation function of the $^{12}C+^{12}C$ system has yield of about 30% of the unitarity limit, assuming a plausible spin assignment $J^\pi=14^+$. This fact again indicates "surface transparency" in the relevant partial wave.

In § 2 a schematic argument will be given for the mechanism of the occurrence of the two-body nuclear molecular resonances. A band crossing diagram as well as the importance of the effective barriers will be explained in detail. The usual coupled-channel formalism will be recapitulated in § 3. The band crossing diagram suggests the cardinal importance of the aligned subchannels in the coupled channel framework. Results will be compared with experiments in § 4. In § 5 discussions will be devoted to the basic character of the imaginary part of the interaction potential in connection with an interpretation of the observed fusion cross section in light heavy-ion reactions. Resonances observed prominently in the rearrangement reaction channels will be discussed in § 6, especially those observed in the lower energy region of the ^{12}C-^{12}C system. A summary is given in § 7.

§ 2. Schematic arguments of the band crossing model

We will start with a review of characteristic features of potential resonances. In phenomenological studies the interactions between heavy-ions are usually described by the local optical potential which has real and imaginary parts. In this section we are concerned mainly with the real part including the Coulomb potential. It has resonances for various orbital angular momenta unless it is too shallow. Their sequence in the Woods-Saxon potential looks like a rotational band at least at the high angular momenta. If we assume the interaction between heavy-ions to be repulsive for the inner region, which is expected from recent microscopic studies of the interaction between composite nuclei,[12),13)] we have a rotational sequence of potential resonances from low to high spins. The moment of inertia of the rotational band is approximately equal to that of a rigid rotor of di-nuclear molecule, which is simply understood by the strong localization of the relative wave function at the nuclear surface, as schematically shown in Fig. 1. The width of a potential resonance is determined essentially by its energy relative to the effective bar-

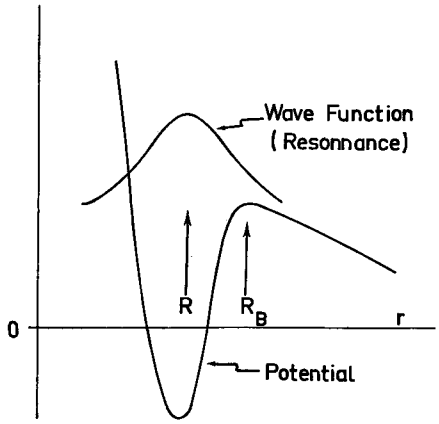

Fig. 1. Illustration of an interaction potential between heavy-ions and a resonance wave function in the potential.

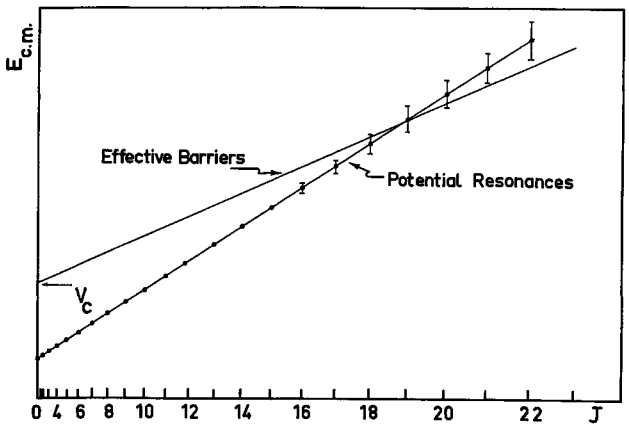

Fig. 2. Characteristics of the band of potential resonances.

rier height for the partial wave, i.e., a resonance well above the effective barrier has a very large width and one well below the barrier has a very small width. As is shown in Fig. 1, the maximum of the radial wave function is located within the effective barrier. This indicates that the resonance energy increases as a function of the angular momentum more rapidly than the hight of the corresponding effective potential barrier. Thus the widths of potential resonances with higher angular momenta are expected to become broader as schematically shown in Fig. 2.

The resonance energies are approximately given by the following expression:

$$E^{(0)}_{J=L}=\frac{\hbar^2}{2\mathcal{J}}\cdot J(J+1)+E_0^{(0)},$$
$$\mathcal{J}\simeq\mu R^2,\quad R=r_0\cdot(A_1^{1/3}+A_2^{1/3}),\qquad(2\cdot1)$$

where μ is the reduced mass, r_0 is the nuclear range parameter taken to be 1.25 fm and A_1, A_2 are the mass numbers of nuclei in the incident channel. On the other hand the heights of the effective potential barriers are given by a similar expression to Eq. (2·1),

$$B^{(0)}_{J=L}=\frac{\hbar^2}{2\mathcal{J}_B}\cdot J(J+1)+V_C(R_B),$$
$$\mathcal{J}_B=\mu R_B^2,\quad R_B=r_0\cdot(A_1^{1/3}+A_2^{1/3})+\Delta R_B,\qquad(2\cdot2)$$

where V_C is the Coulomb potential between heavy ions. R_B is the position of the top of the effective potential barrier under the presence of the attractive nuclear interaction. More exactly, the contribution from the nuclear interaction should be added to the right-hand side of the first equation of Eq. (2·2). As a rough estimate, ΔR_B is taken as 1.5 fm for light heavy ion systems. This gives different slopes to the $J(J+1)$-plots for the energies of resonances and barrier tops which results in a crossing as schematically shown in Fig. 2, where $E_0^{(0)}$ is assumed to be smaller than V_C (the Coulomb barrier), i.e., the nuclear interaction is assumed to be attractive enough to have resonances. The feature that the resonance widths increase as the orbital angular momenta or the energies increase is important for the overall energy dependence of the resonance phenomena, as will be seen later. It is pointed out here that the effective local potential between composite nuclei derived from a microscopic theory is known to have an L-dependent attraction in the surface region, together with a repulsive soft core in the inner region.[19] Such an L-dependence gives more attraction for higher partial waves, and thus a smaller slope in the $J(J+1)$-plot of the resonance energies in Fig. 2. This means a possible persistency of narrower potential resonances at higher spins than expected from simple state independent local potentials. Actually the ^{16}O-^{16}O system has been shown to have rather narrow potential resonances up to about $L=20$, as is given in detail in Chapter V. Another important feature of potential resonances is that we cannot have two resonances with the same spin and parity, within an energy range of the oscillation $\hbar\omega$ of the relative wave function. This energy range depends on the reduced mass and the potential adopted and is more than several MeV for combinations of light heavy-ions. Even if we assume a deeper potential such as one obtained by the density folding,[20] we will only have additional deeply bound rotational bands in the potential.

We will proceed to the discussion of the problem of how we can expect resonances due to excitations of some collective states of the target or the

projectile nucleus. It would be worthwhile discussing it carefully, because the coupling to collective intrinsic excitations is usually expected to cause not resonances but rather a continuous flux flow to inelastic channels and then the effects should vary smoothly with energy. Nogami has proposed a picture for a possible mechanism which would cause resonance behavior. We will consider the problem further along this line. We assume that the potential in the elastic channel is attractive enough to have bound or quasi-bound states. Almost the same bound or quasi-bound states will exist in the inelastic channels, if the interaction potentials in the inelastic channels are almost the same as that in the elastic channel. The energies of such states are, of course, raised from their original positions by the amounts of excitation energies of the target or the projectile nucleus as shown in Fig. 3. Usually people expect that the resonances will be observed at these energies in the elastic and in the inelastic scattering. These states are, however, not always observed as resonances. Whether they are observed as resonances or not depends crucially on the couplings between the relevant channels. In other words, a state has to share an appropriate amount of the partial width of the entrance channel as well as that of the exit channel in order to be observed as a resonance, as is seen in the Breit-Wigner formula,

$$\sigma(E) \approx \pi \cdot \lambda\!\!\!^{-2} \cdot \frac{\Gamma_{\text{exit}} \cdot \Gamma_{\text{ent}}}{(E-E_R)^2 + \Gamma^2/4}, \qquad (2\cdot3)$$

where the total width Γ of the resonance should be narrow enough. As a matter of course the magnitudes of the partial width shared among resonances depend on the strength of the coupling interaction. At the same time, however, they also depend on the relative distance between the positions of the original resonances. Let us consider a bound state problem in which there are two unperturbed states near to each other. If there exists a coupling interaction, it causes a strong mixing between them. Then we will have two states which have their original components shared as the result of the interaction. If such a situation occurs in a scattering process, that is, if a bound or quasi-bound state in some channel is close to a resonance in the incident channel, then we will observe two resonances which have approximately half of the single particle widths of the elastic and of the considered channel. In the case where the width of a resonance in the incident channel is broad, we will observe a gross structure behavior with intermediate resonances superimposed on it. This is the case that Scheid et al.[9] called double-resonance mechanism. A problem which remains is how to predict at what energies or with what spin values such situations will occur.

Where an excited state of the target or the projectile has a spin I not equal to zero (here we assume the ground state spin to be zero), there is a very interesting feature in the series of potential resonances in the

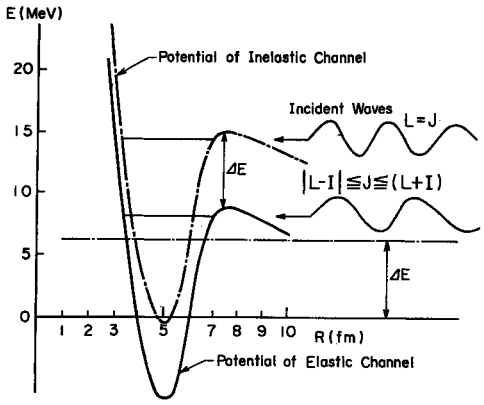

Fig. 3. Illustration of Nogami's picture. An incident particle falls into the potential pocket by loosing the relative energy due to an intrinsic excitation, which implies the existence of degenerate quasi-stationary states with $|I-L| \leq J \leq I+L$ at an energy higher than the original potential resonance by ΔE.

inelastic channel. As is seen in Fig. 3, for each resonance with orbital angular momentum $L=J$ in the incident channel, we have degenerate multiplet states with the total spins $J=|L-I|, \cdots, L+I$ in the inelastic channel. All of them will not necessarily be observed as actual resonances as discussed above. In order to see whether they come close to the resonances in the elastic channel, we plot the energies of these states versus $J(J+1)$, together with the potential resonances in the elastic channel given by Eq. (2·1). Figure 4 shows the case of the ^{12}C-^{16}O system with 3^- (6.13 MeV) excitation of the ^{16}O nucleus. Their possible total spins in the inelastic channel are $J=|L-3|, |L-1|, L+1, L+3$ with parity selection $\pi=(-)^J$ required by the incident channel. Each of them forms a quasi-rotational band. It should be noted that one of them, the aligned rotational band, gets close to the elastic molecular rotational band and even across over it at a certain high spin and energy.

Energies of the quasi-rotational bands are given as follows,

$$E_J^{(1)} = \frac{\hbar^2}{2\mathcal{J}} L(L+1) + \Delta E_1 + E_0^{(0)},$$
$$L = |J-I|, \cdots, J+I. \qquad (2\cdot4)$$

Then those of the aligned rotational band are

$$E^{(1)}_{J=L+I} = \frac{\hbar^2}{2\mathcal{J}} (J-I)\cdot(J-I+1) + \Delta E_1 + E_0^{(0)}. \qquad (2\cdot5)$$

We can easily estimate the crossing point by using Eqs. (2·1) and (2·5). For example, the 3^- excitation of the ^{16}O nucleus with ΔE_1 equal to 6.13 MeV gives the crossing spin value,

$$J_{\text{cross}} = \frac{1}{2}\cdot\frac{\Delta E_1}{(\hbar^2/2\mathcal{J})\cdot I} + \frac{1}{2}\cdot I - \frac{1}{2} \approx 13, \qquad (2\cdot6)$$

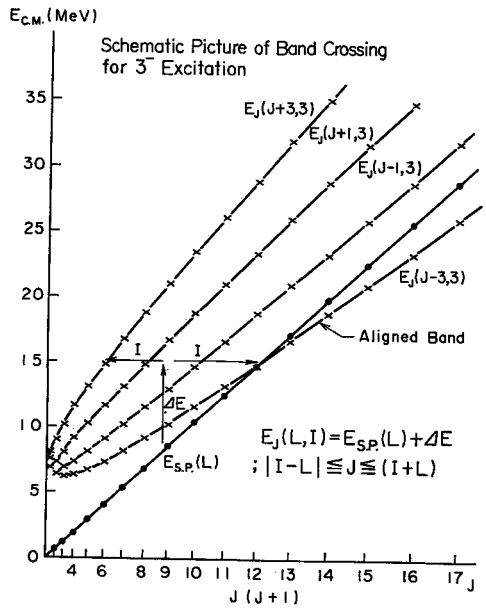

Fig. 4. Schematic diagram of the crossing of the elastic and the inelastic aligned molecular bands in the case of $^{16}O^*$ (3^-, 6.13 MeV) excitation. $E_{s.p.}(0)$, i.e., an energy of S-wave potential resonance, is assumed to be 0.0 MeV, for simplicity.

where r_0 in Eq. (2·1) is assumed to be 1.25 fm.

As discussed above, around the crossing point where two resonance states are close to each other there will be strong mixing between the members of the two rotational bands, and then there will occur prominent resonance phenomena in both elastic and inelastic scattering. From this schematic argument we can easily estimate the region of molecular resonances, where the observation condition discussed above is fulfilled. The absolute values of the resonance energies depend on $E_0^{(0)}$, the band head energy of the elastic molecular band. Indicative experimental data or microscopic calculations might be necessary, but in practice the energy region for observable potential resonances is rather strictly limited for each partial wave, because the partial width crucially depends on the effective barrier height as discussed below.

Other important aspects to be discussed concerning the observation are the original widths of potential resonances. First the original width of a potential resonance is determined mainly by its relative position to the effective barrier top. Only around the barrier top energy does the resonance have an appropriate width which is not too small and not too large. Thus the molecular resonance region is expected to be limited around the effective potential barrier for each partial wave. Secondly there exist differences in the widths of the elastic and of the inelastic potential resonances with the same total spin (not with the same orbital angular momentum). This indicates the possibility that there might exist a resonance whose width is sharper than that of the potential resonance in the elastic channel. The total width of a resonance is given in the

zeroth order estimation as follows:

$$\Gamma = a \cdot \Gamma_0^{\text{s.p.}} + (1-a) \cdot \Gamma_1^{\text{s.p.}} + \Delta\Gamma\,, \tag{2·7}$$

where $\Gamma_i^{\text{s.p.}}$ is the single-particle width in the channel i and a denotes the mixing ratio between the elastic and the excited molecular resonances. $\Delta\Gamma$ represents effects of the other reaction processes, which are expected to be small over a certain energy region as discussed in § 1. As $\Gamma_1^{\text{s.p.}}$ is smaller than $\Gamma_0^{\text{s.p.}}$ for the aligned rotational band, then the total width Γ can be smaller than $\Gamma_0^{\text{s.p.}}$. The smallness of $\Gamma_1^{\text{s.p.}}$ compared with $\Gamma_0^{\text{s.p.}}$ can be seen again by the schematic diagram for the effective barriers. The barrier heights in the inelastic channel are given by the following formula,

$$B_J^{(i)} = \frac{\hbar^2}{2\mathcal{J}_B} \cdot L(L+1) + V_C(R_B) + \Delta E_i\,,$$
$$L = |J-I|, \cdots, J+I\,. \tag{2·8}$$

In Fig. 5, a schematic diagram of the effective barriers for the elastic and for the aligned sub-channels is given for the ^{12}C-^{16}O system with the ^{16}O*(3^-, 6.13 MeV) excitation. We can see that $B^{(1)}_{J=L+3}$ is higher than $B^{(0)}_{J=L}$ except in the very high energy region.

In the above paragraphs qualitative arguments for the BCM have been illustrated with the 3^- (6.13 MeV) excitation of ^{16}O in the ^{12}C+^{16}O system. The same arguments can be made for the ^{12}C-^{12}C and ^{16}O-^{16}O systems with one or combined excitations of the 2_1^+ (4.44 MeV) and the 3_1^- (9.64 MeV) states in the ^{12}C nucleus and the 3^- (6.13 MeV) and the 4_1^+ (10.35 MeV) states, etc. in the ^{16}O nucleus. The crossings between the elastic and the inelastic mole-

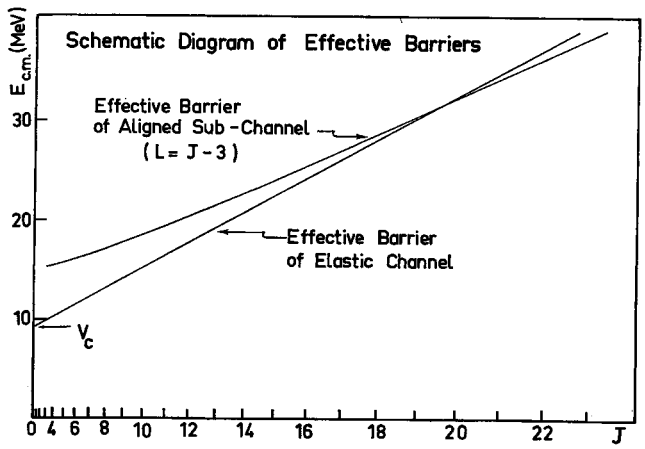

Fig. 5. Schematic diagram of the effective barriers between the elastic channel and the inelastic aligned channel in the case of ^{16}O*(3^-, 6.13 MeV). A spin at the crossing point is higher than that of the molecular bands as shown in Fig. 4.

cular bands are seen at certain total spin values, depending on the intrinsic spins and the excitation energies. It should be stressed here that the arguments can be made without any arbitrary parameter or without any artificial assumption.

Notice here that an aligned molecular configuration with an intrinsic excitation will appear as the dominant component of observed resonances. In other words we will observe selectively one type of coupling between the intrinsic spin and the orbital angular momentum. Further the dominant component itself will change among various excitations of heavy-ions as the spins and the energies increase, according to the differences in crossing points of their aligned molecular bands with the elastic one.

§ 3. Formulation

According to the schematic arguments of the BCM, the aligned sub-channels of inelastic channels will play an essential role in the two-body nuclear molecular resonances. More precisely the potential resonances in the aligned inelastic sub-channels can be close to those in the elastic channel in some region around the crossing points. In order to perform a quantitative study of resonance phenomena based on the picture of the BCM, we use the framework of the coupled-channel method.[21]

3.1. *Coupled channel equation*

The total Hamiltonian is assumed to have the following form,

$$H = h_1(\theta_1) + h_2(\theta_2) + T(\boldsymbol{r}) + U(\boldsymbol{r}, \theta_1, \theta_2), \tag{3·1}$$

where $h_i(\theta_i)$ is the internal Hamiltonian with internal variables θ_i of the i-th nucleus. $T(\boldsymbol{r})$ and $U(\boldsymbol{r}, \theta_1, \theta_2)$ are the kinetic operator and the interaction potential for the relative motion between nuclei. The internal wave function $\chi_{I_iM_i}(\theta_i)$ is assumed to be an eigenfunction of the internal Hamiltonian $h_i(\theta_i)$,

$$h_i(\theta_i) \cdot \chi_{I_iM_i}(\theta_i) = \varepsilon_{I_i} \cdot \chi_{I_iM_i}(\theta_i), \tag{3·2}$$

where I_i and M_i are the internal spin and its projection, respectively. ε_{I_i} is an energy eigenvalue. For simplicity we use the abbreviated index c which represents the channel for a total spin J,

$$c \equiv ((I_1, I_2) I, L). \tag{3·3}$$

The total wave function Ψ_{JM_J} of the system is written as

$$\Psi_{JM_J}(\boldsymbol{r}, \theta_1, \theta_2) = \sum_c \frac{u_c(r)}{r} \cdot \mathcal{Y}_c^{JM_J}(\hat{\boldsymbol{r}}, \theta_1, \theta_2), \tag{3·4}$$

where

$$\mathcal{Y}_c^{JM_J}(\hat{\boldsymbol{r}}, \theta_1, \theta_2) = \sum_{\substack{M_1 M_2 \\ M_I M_L}} (I_1 M_1 I_2 M_2 | I M_I) \cdot (I M_I L M_L | J M_J) \cdot Y_{LM_L}(\hat{\boldsymbol{r}}) \cdot \chi_{I_1 M_1}(\theta_1) \cdot \chi_{I_2 M_2}(\theta_2) . \tag{3·5}$$

The $u_c(r)$ and $Y_{LM_L}(\hat{\boldsymbol{r}})$ are the usual radial part and angular part of the relative wave function with angular momentum L and its projection M_L. In the collision of identical nuclei, for example, the $^{12}C+^{12}C$ and $^{16}O+^{16}O$ systems, the channel wave function $\mathcal{Y}_c^{JM_J}$ should be symmetrized.

Multiplying $\mathcal{Y}_c^{JM_J*}(\hat{\boldsymbol{r}}, \theta_1, \theta_2)$ to the Schrödinger equation $(H-E)\Psi_{JM_J}=0$, and integrating over the variables $\hat{\boldsymbol{r}}$, θ_1 and θ_2 we obtain the coupled-channel equation for the radial wave functions,

$$\sum_{c'} [(\mathcal{L}_c(r) - E_c)\delta_{cc'} + v_{cc'}(r)] u_{c'}(r) = 0 , \tag{3·6}$$

where

$$\mathcal{L}_c(r) = -\frac{\hbar^2}{2\mu}\left(\frac{d^2}{dr^2} - \frac{L_c(L_c+1)}{r^2}\right) + U_c(r) . \tag{3·7}$$

E_c is the energy of relative motion in the channel c; $E_c = E - \varepsilon_{I_1} - \varepsilon_{I_2}$. μ is the reduced mass of the system. $U_c(r)$ is the diagonal part of the interaction potential in the channel c and $v_{cc'}(r)$ is the coupling potential between channels given in Eq. (3·17).

3.2. *Diagonal part of the interaction potential*

The interaction in the present study is described phenomenologically by the use of local potentials. The diagonal part is the sum of the nuclear and Coulomb potentials,

$$U_c(r) = U_c^{\text{nuclear}}(r) + U^{\text{Coulomb}}(r) + iW(r) . \tag{3·8}$$

The imaginary part is added to describe the absorption due to other reaction channels which are not included in the coupled-channel model space. The nuclear part is assumed to be attractive at long distances and to be repulsive at short distances. The repulsive core at short distances is a phenomenological representation of the effects of the Pauli principle between composite nuclei. The long range part is described by the Woods-Saxon form throughout the present paper. The short range part is represented by the Woods-Saxon or Gaussian form. It is shown in the next section that both forms work equally well in order to set up a series of bound or quasi-bound states similarly to the results of microscopic studies.

$$U_c^{\text{nuclear}}(r) = V_{\text{core}} \cdot f_{\text{core}}(r, a_{\text{core}}, R_{\text{core}}) + V_c \cdot f_{\text{WS}}(r, a, R_0) , \tag{3·9}$$

where $f_{\rm WS}$ is the Woods-Saxon form factor, $f_{\rm core}$ is a repulsive core function and the factors $V_{\rm core}$ and V_C are the strengths of the core and attractive parts, respectively.

We adopt the usual form for the Coulomb potential,

$$U^{\rm Coulomb}(r)=\begin{cases}\dfrac{3}{2}\dfrac{z_1z_2e^2}{R_c}\cdot\left(1-\dfrac{1}{3}\dfrac{r^2}{R_c^2}\right), & r\leq R_c\,,\\ \dfrac{z_1z_2e^2}{r}, & r\geq R_c\,,\end{cases} \tag{3·10}$$

where R_c is the radius where two spheres of uniform charge just touch, namely $R_c=R_{c_1}+R_{c_2}$ with $R_{c_i}=r_{0c}A_i^{1/3}$. r_{0c} is taken to be 1.25 fm.

The imaginary part should guarantee the "surface transparency" or the weak absorption for grazing partial waves as mentioned in § 1. We have therefore adopted the Woods-Saxon form of angular-momentum dependence proposed by Chatwin, Eck, Robson and Richter,[10b]

$$W(r)=W_0\cdot\frac{1}{1+\exp[(J-J_c)/\Delta J]}\cdot f_{\rm WS}(r,a,R_0)\,, \tag{3·11}$$

where W_0 is the strength and the radial form is taken to be the same as the long range part of the real nuclear potential. The transition region from strong to weak absorption is adjusted by the diffuseness parameter ΔJ. The critical angular momentum J_c is defined as follows in the present study,

$$J_c=\left(\frac{2\mu}{\hbar^2}\right)^{1/2}\cdot\bar{R}\cdot(E_{\rm c.m.}+\bar{Q})^{1/2}, \tag{3·12}$$

where $\bar{R}$ and $\bar{Q}$ are called the effective interaction range and the effective Q-value for possible reaction processes, respectively. If $\bar{R}$ is chosen to be R_B and $\bar{Q}$ to be $-V_C(R_B)$ in Eq. (2·2), J_c becomes the grazing angular momentum J_g. The parameters $\bar{R}$ and $\bar{Q}$ should be chosen to give $J_c<J_g$ for a certain energy region so as to guarantee the existence of a surface transparent region. Justification for the values of $\bar{R}$ and $\bar{Q}$ will be discussed in § 5 in connection with recent development in understanding the observed fusion cross sections in heavy-ion reactions.

3.3. *Coupling interactions*

The coupling interactions between the elastic and the inelastic channels are derived phenomenologically. We assume the internal motion of the target or projectile to be described by the collective model for simplicity. For the rotational motion, the internal wave function is described by an axially symmetric rotor motion,

$$\chi_{IM}(\theta)=\sqrt{\frac{2I+1}{8\pi^2}}\cdot D^I_{M,0}(\theta)\,, \tag{3·13}$$

where the internal variable θ is a set of the Euler angles. For the vibrational motion,

$$\chi_{IM}(\theta) = b^{\dagger}_{IM}|0\rangle , \tag{3·14}$$

where $b^{\dagger}_{IM}$ is the usual phonon creation operator. The vibrational amplitude parameter α_{IM} is represented as usual,

$$\alpha_{IM} = \frac{\gamma_I}{\sqrt{2I+1}}(b_{IM} + (-)^M b^{\dagger}_{IM}), \tag{3·15}$$

where γ_I is the strength parameter.

Coupling interactions among the elastic and the inelastic channels are induced by variations of interaction ranges in the long range attractive part of interaction potentials between heavy-ions, due to the collective surface oscillations of heavy ions.

$$R = \sum_i \begin{cases} R_i \cdot (1 + \beta_2 \cdot Y_{20}(\Omega_i')), \\ R_i \cdot (1 + \sum_{\mu} \alpha_{3\mu} \cdot Y_{3\mu}(\hat{r})), \end{cases} \tag{3·16}$$

where $R_i = r_0 \cdot A_i^{1/3}$, β_2 is the deformation parameter, and the angle Ω_i' refers to the body fixed frame of the ^{12}C nucleus. The summation $\sum_i$ is taken depending on which combination of ^{12}C and ^{16}O nuclei is considered. We retain only the first order terms of the expansion of the Woods-Saxon potential in powers of $\beta_2 Y_{20}(\Omega_i')$ and $\sum_\mu \alpha_{3\mu} Y_{3\mu}(\hat{r})$ and get the following form:

$$V(\boldsymbol{r}, \theta_1, \theta_2) = V_C \sum_i \begin{cases} g(r, R_i) \cdot \beta_2 \cdot Y_{20}(\Omega_i'), \\ g(r, R_i) \cdot \sum_{\mu} \alpha_{3\mu} Y_{3\mu}(\hat{r}), \end{cases}$$

$$v_{cc'}(r) = \langle {}^{Q}\mathcal{Y}_c^{JM_J} | V(\boldsymbol{r}, \theta_1, \theta_2) | {}^{Q}\mathcal{Y}_{c'}^{JM_J} \rangle , \tag{3·17}$$

where $\sum_i$ should be take in the same ways as in Eq. (3·16). The function $g(r, R_i)$ is the radial form factor of the coupling interaction and is given by the derivative of f_{WS}.

$$g(r, R_i) = \frac{R_i}{a} \cdot \frac{\exp[(r - R_0)/a]}{\{1 + \exp[(r - R_0)/a]\}^2} , \tag{3·18}$$

where $i = 1$ or 2, specifies heavy-ion and $R_0 = R_1 + R_2$. In the case of the 2^+ (4.44 MeV) excitation of the ^{12}C + ^{12}C system, we include the second order terms of the expansion. The inclusion does not change the essential features of the resonance cross sections.

Recently the interactions between heavy-ions have been calculated by density folding. Diagonal potentials are very deep and coupling interactions are also rather strong. The stronger couplings between the elastic and the inelastic channels than those adopted here might produce quantitative differences. For example, resonance energies obtained after coupling might be shifted from the

original potential resonance positions by larger amounts than obtained here. But the basic resonant mechanism is not changed at all. The Pauli exchange effects have been known to exert a great influence on interaction between composite nuclei, especially in the inner region, as given in detail in Chapter V. An effective local interaction derived from microscopic calculations is shown to be much weaker than the folded potential. A coupling interaction obtained by the folding model would be strongly affected by the inclusion of the Pauli exchange effects.

3.4. *Method for solving the coupled-channel equation*

The coupled-channel equation (3·6) is solved by the use of the Kohn-Hulthen[22] type variational method which has been developed by Mito and Kamimura.[23] They have proposed a simple and useful method for solving the one channel scattering equation based on the variational method by utilizing the generator coordinate method for the choice of the trial wave function. We have extended Mito and Kamimura's method to the many channels' problem following Mott and Massey.[24] As the trial wave function, we use the localized Gaussian form. The details are given in Refs. 14f) and 25).

3.5. *Cross sections*

We calculated the differential cross sections and angle-integrated cross sections by using elements of the S matrix which are obtained by solving the coupled-channel equation (3·6) at each incident energy. The differential cross section is given in the usual way by the following equation:

$$\frac{d\sigma_{c'c}}{d\Omega_{c'}}=\frac{1}{(2I_1{}^c+1)\cdot(2I_2{}^c+1)}\cdot\frac{v_{c'}}{v_c}\sum_{\substack{I_cM_c\\I_{c'}M_{c'}}}\Bigg|f^{(c)}_{\mathrm{Coul}}(\Omega_{c'})\delta_{cc'}$$
$$+\frac{i}{2k_c}\cdot\sqrt{\frac{v_c}{v_{c'}}}\sum_{\substack{L_cM_{L_c}\\L_{c'}M_{L_{c'}}\\JM_J}}4\pi i^{L_c-L_{c'}}\cdot(I_cM_cL_cM_{L_c}|JM_J)$$
$$\cdot(I_{c'}M_{c'}L_{c'}M_{L_{c'}}|JM_J)$$
$$\cdot\exp(i(\sigma_{L_c}+\sigma_{L_{c'}}))$$
$$\cdot[\delta_{cc'}-S^J_{cc'}]\cdot Y_{L_{c'}M_{Lc'}}(\Omega_{c'})\cdot Y^*_{L_cM_{L_c}}(\Omega_c)\Bigg|^2, \qquad (3\cdot19)$$

where $f^{(c)}_{\mathrm{Coul}}$ denotes the Coulomb scattering amplitude and σ_{L_c} is the Coulomb phase shift.

We also calculate the angle-integrated cross section for inelastic scattering, by the following expression:

$$\sigma_{c'c}(E_{\mathrm{c.m.}})=\frac{\pi}{k_c{}^2}\sum_{\substack{I_cI_{c'}\\L_cL_{c'}J}}g_J\cdot|S^J_{c'c}|^2, \qquad (3\cdot20)$$

where g_J is the statistical factor,

$$g_J = \frac{2J+1}{(2I_1{}^c+1)\cdot(2I_2{}^c+1)} . \tag{3·21}$$

The total reaction cross section σ_R is defined as the total flux loss from the elastic channel and is given as follows,

$$\sigma_R(E_{\text{c.m.}}) = \frac{\pi}{k_c{}^2}\sum_{L_cI_cJ} g_J(1-|S_{cc}^J|^2), \tag{3·22}$$

where S_{cc}^J is the element of the S-matrix for the elastic channel.

The fusion cross section is defined in the present study as the difference between the total reaction cross section and the total inelastic cross section (including all inelastic channels) and is given by the following equation:

$$\sigma_{fus}(E_{\text{c.m.}}) = \sigma_R(E_{\text{c.m.}}) - \sum_{c'\neq c}\sigma_{c'c}(E_{\text{c.m.}}) . \tag{3·23}$$

In the case of scattering between identical nuclei, the equations (3·19), (3·20), (3·22) and (3·23) should be modified to take symmetry into account. This modification produces extra factors and limitations on the summation of the angular momentum. The total reaction cross section for scattering of two identical spinless particle, for example, becomes as follows,

$$\sigma_R{}^{\text{sym}}(E_{\text{c.m.}}) = \frac{2\pi}{k_c{}^2}\sum_J^{\text{even}}(2J+1)(1-|S_{cc}^J|^2) . \tag{3·24}$$

§ 4. Results

In this section we give the results of the numerical calculations and see how the BCM explains and reproduces general trends of the experimental data, i.e., widths and yields of a series of resonances observed in the excitation functions of the elastic and the inelastic scattering. The ^{12}C-^{12}C, ^{16}O-^{16}O and ^{12}C-^{16}O scattering in the energy region well above the Coulomb barrier will be discussed as mentioned in § 1. Resonances in other reaction channels, in other energy regions and in other systems will be discussed in § 6.

4.1. *^{12}C-^{12}C scattering*

We show a band crossing diagram for the ^{12}C+^{12}C system in Fig. 6. It includes the excitation of the $2_1{}^+$(4.44 MeV), the $0_2{}^+$(7.65 MeV), the $3_1{}^-$(9.64 MeV) and the $4_1{}^+$(14.08 MeV) states and in some cases mutual excitations. In the elastic molecular band we use the value 1.25 fm for r_0 in Eq. (2·1) and assume the band head energy $E_0{}^{(0)}$ in Eq. (2·1) to be 6.0 MeV according to the result of our previous analysis of the sub-Coulomb resonances,[8] which will be given in § 6. As is clearly shown in the figure, the $2_1{}^+$, $3_1{}^-$ and $4_1{}^+$ excited bands cross the elastic molecular band in the regions of $J^\pi = 10^+ \sim 12^+$, $\sim 16^+$ and $\sim 18^+$, respectively. The aligned rotational

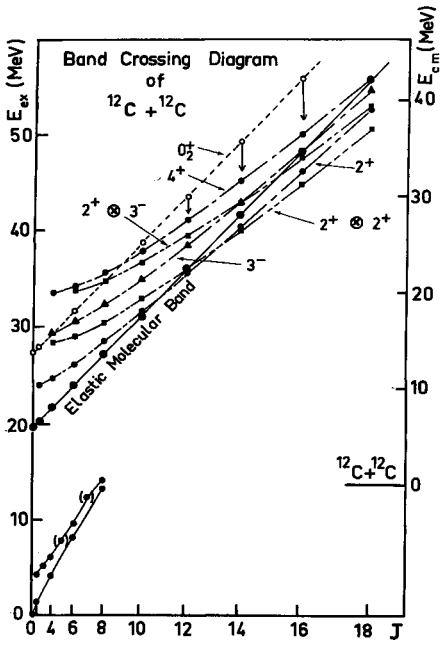

Fig. 6. Band crossing diagram of the $^{12}C+^{13}C$ system. Only aligned molecular bands are shown among excited bands. Open circles are resonance energies with an excitation of a clustering state and arrows attached indicate possible shifts due to a change in an interaction potential as explained in the text. Squares mean the mutual excitations and triangles the 3^- excitation.

bands in the mutual 2_1^+ excitation channel and in the 2_1^+ and 3_1^- excitation channel (in which the channel spins are 4^+ and 5^- respectively) also cross the elastic band at about $J^\pi = 12^+ \sim 14^+$ and $14^+ \sim 16^+$ respectively in spite of their high excitation energies (8.88 MeV and 14.08 MeV). On the other hand, the 0_2^+ excited band (which, of course, is unique because of the zero intrinsic spin) does not cross the elastic band at all. We should, however, take into account a possible change in the interaction between the ^{12}C nuclei in the excited 0_2^+ state, because this involves a drastic change in structure, i.e., a change to a spatially extended 3α-cluster structure. This might result in a longer interaction range, which will give rise to a larger moment of inertia than that of the elastic molecular band. (The simple band crossing diagram assumes no change in the interaction between heavy-ions under their intrinsic excitations, which is reasonable for excitations without any large structure change.) The arrows in Fig. 6 suggest a possible shift of the resonance positions due to the change of interaction in the excited state. In order to determine qualitatively the shift, one has to investigate the interaction by carefully taking into account the structure change in the ^{12}C nucleus.

Effectively it is found by experiment that both the single and the mutual 2_1^+ inelastic cross sections show prominent resonances in the energy region where the corresponding aligned rotational bands approach and cross the elastic one. Of course whether members of these bands may or may not produce discernible peaks in the cross section comparable with experiment depends on

the magnitudes of the widths of the original resonances which couple with each other.

Another important prediction of the BCM is the systematic change of the dominant inelastic excitation component of the resonances as the energy and the angular momentum increase. This prediction is illustrated in Fig. 6. The dominant component of the resonances is expected to change systematically from the single and mutaual 2_1^+ excitations to the 3_1^- excitation (single and mutual with the 2_1^+) and finally to the 4_1^+ excitation at angular momenta in the range of $10\sim18\,\hbar$. This prediction has been proved by a recent experiment.[26]

We will now consider the problem of dynamical couplings among members of molecular bands in scattering process. The model space of the present calculation is composed of the following sub-channels:

i) the elastic channel; $I_c=0,\ J=L,$

ii) the singe 2_1^+ excitation; $I_c=2,\ J=L+2,\ L,$

iii) the mutual 2_1^+ excitation; $I_c=4,\ J=L+4,\ L+2,$

iv) the mutual 2_1^+ excitation; $I_c=2,\ J=L+2,$

v) the single 3_1^- excitation; $I_c=3,\ J=L+3,\ L+1.$

Although we have included several additional sub-channels, other than the aligned sub-channels, the resonance cross sections are essentially determined by the latter. The potential parameters are chosen so that there is a potential resonance with spin 12 at about $E_{\text{c.m.}}=20.0$ MeV. We obtain an additional molecular band with one radial node. Only the low spin members of it have widths suitable for observation (not too large). The 2^+ member is located at about $E_{\text{c.m.}}=6.3$ MeV, which is consistent with the fragmentation analysis of the sub-Coulomb resonances,[8] as will be explained in § 6. We have not assumed any state-dependent potential, like that which emerges from the microscopic studies, but by finely varying the depth parameters of the attractive potentials the observed resonance energies can be better reproduced. The values of the potential parameters are listed in Table I.

Table I. The potential parameters of the $^{12}C+^{12}C$ system. The part indicated "core" represents a short range repulsive soft core reflecting the effects of the Pauli principle, where the Woods-Saxon functional form is assumed. The depths of the long range attractive potential are given by V_1, V_2, V_3 and V_4 for the elastic, single 2_1^+, mutual 2_1^+ and single 3_1^- inelastic channels, respectively. According to Eqs. (3·11) and (3·12), the parameters W_0, $\bar{R}$, $\bar{Q}$ and ΔJ define the imaginary part. β_2 and γ_3 stand for the coupling parameters to the 2_1^+ and 3_1^- excitations, respectively.

Core Part			Attractive Part						Imaginary Part				Coupling	
V_{core} (MeV)	R_{core} (fm)	a_{core} (fm)	V_1 (MeV)	V_2 (MeV)	V_3 (MeV)	V_4 (MeV)	R_0 (fm)	a (fm)	W_0 (MeV)	$\bar{R}$ (fm)	$\bar{Q}$ (MeV)	ΔJ (N.D.)	β_2 (N.D.)	γ_3 (N.D.)
100.0	2.4	0.3	−17.0	−16.0	−15.0	−17.0	5.72	0.35	−7.0	5.72	−12.0	1.0	−0.3	0.15

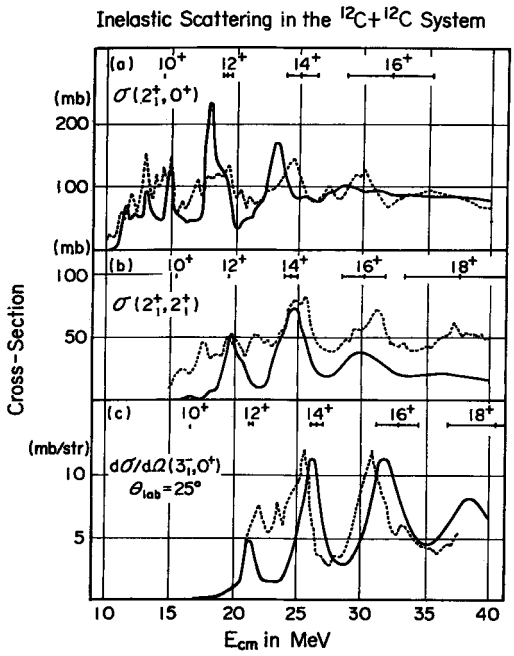

Fig. 7. Inelastic cross sections in the $^{12}C+^{12}C$ system. Single 2_1^+, mutual 2_1^+ and single 3_1^- inelastic cross sections are shown in parts (a), (b) and (c), respectively. The solid lines show the results of our calculations. The adopted potential parameters are those of Table I. The dotted lines show experimental data (Refs. 15), 27)). In the upper part of each panel, the predicted energies and widths of the zeroth order resonances in each inelastic aligned channel, which are calculated without coupling and absorption effect, are shown with their spins and parities.

Our calculated inelastic cross sections are shown in Fig. 7 and are compared with experimental data.[15),27)] The angle integrated cross sections for single and mutual 2_1^+ inelastic scattering are shown in panels (a) and (b), respectivley. This figure clearly shows that the calculation reproduces resonance structures for all three inelastic channels, as is expected from the discussion of §2. An important point is that the calculated cross sections properly reproduce the resonance energies, widths and yield of the observed resonances for all three inelastic scattering channels. Each peak of the cross section corresponds to one partial wave, i.e., the peaks at about $E_{c.m.}=20$, 25 and 30 MeV correspond to partial waves with J^π equal to 12^+, 14^+ and 16^+, respectively.

Recently Fulton, Cormier and Herman[28)] have pointed out that while the model is in reasonable overall agreement with many features of the data, it seems to be incomplete. The calculations, in particular, consistently underpredict the amount of fragmentation of the gross structure resonances. Other degrees of freedom might take part in the observed resonances and might play an essential role in some of them. The problem of other degrees of freedom will be discussed in § 6 along the viewpoint of the BCM extended to rearrangement channels. It is, however, necessary to notice here that these calculations do not include any of the mutual excitation of the 2_1^+ and the 3_1^- states of the ^{12}C nucleus. The importance of the corresponding aligned band is recongnized in Fig. 6 at spins larger than 14^+, where it crosses with the

elastic and the 3^- aligned molecular bands. In this region the component of the mutual $(2_1^+, 3_1^-)$ excitation will mix with resonances whose main components are those of the elastic and the single 3^- excitation channels, and further there should be additional resonances with a dominant component of the mutual excitation although its direct coupling potential with the incident channel might be weak. Thus we can expect more fragmentations and sharper widths as discussed in § 2. As for the 0_2^+ inelastic channel we should be careful in drawing a schematic diagram, because the 0_2^+ state has been shown to have a longer root-mean-square radius than the ground state and thus the interaction between the ^{12}C nuclei might be different from that in the ground state, as is mentioned at the beginning of this sub-section. Of course, as the 0_2^+ state of ^{12}C is known to have a well-developed 3α-cluster structure as mentioned in Chapter II, one might claim that the α-particle degrees of freedom are important for resonances which have a large partial width for the 0_2^+ inelastic channel.

In the upper part of each panel in Fig. 7, the energies and widths of the zeroth order resonances in each inelastic channel are shown. The calculated resonance peaks roughly correspond to the original potential resonances in each channel. Multiplet resonances do not clearly appear in this calculation except for spins lower than 12. This just corresponds to the experimental data. This is different from the case of the ^{12}C-^{16}O system, where clear multiplet-like resonances were observed especially in the ^{16}O*$(3^-, 6.13\,\mathrm{MeV})$ inelastic channel,[16e] as will be discussed later in this section. One of the possible explanations for the absence of multiplet structure is the overlapping of wide resonances which couple to each other. We have observed the transition from multiplet to single peak structure in a simple model calculation where the widths of the two resonances to be coupled have been changed systematically. In this calculation, our model space is truncated to include only the elastic and single 2_1^+ inelastic channels so that only the coupling between two resonances is involved. All the potential parameters assumed are identical to those in Table I except for the depths of the attractive potentials V_1 and V_2. To examine the coupling between resonances with various widths, we have considered three cases, i.e., $V_1 = V_2 = 21$ MeV, 19 MeV and 17 MeV, respectively. The calculated inelastic cross sections for $J^\pi = 14^+$ are shown in Fig. 8. In the upper part of each panel the energies and the widths of the zeroth order resonances in the elastic and in the inelastic channels are shown. The three panels of Fig. 8 show a gradual change from doublet to a wider single peak depending of course upon the widths of resonances to be coupled. As is expected the coupling between narrow resonances produces doublet peaks. In the limit, coupling between wide resonances produces a single peak. Another possible explanation of the absence of multiplet structures would be the existence of a strong absorption region at energies a little higher than the ob-

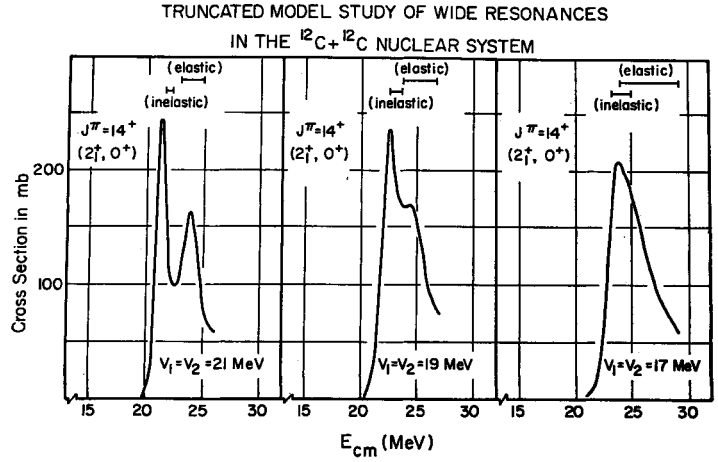

Fig. 8. Coupling between two resonances with various widths. Integrated inelastic cross sections for a partial wave $J^{\pi}=14^+$ are shown for the coupling between two resonances in the elastic and single 2_1^+ inelastic channels. The three panels correspond to the cases, $V_1=V_2=21.0$, 19.0 and 17.0 MeV, respectively. For the model space and other parameters see the text. In the upper part of each panel the energy and width of the zeroth order resonances in the elastic and single 2_1^+ inelastic channels are shown. Comparison among the three panels shows a gradual change from doublet peaks to a single wide peak.

served resonances for each partial wave. The upper member of the multiplet is pushed up by the interaction with the lower resonance and would fall into the region. Which explanation is realistic is yet to be clarified. (The calculated results shown in Fig. 7 include both effects.)

4.2. ^{16}O-^{16}O *scattering*

Figure 9 shows a band crossing diagram for the ^{16}O-^{16}O system, including the excitations of the 3_1^- (6.13 MeV), the 0_2^+ (6.05 MeV), the 2_1^+ (6.92 MeV) and the 4_1^+ (10.35 MeV) states and the mutual excitations of some of them. The band head energy $E_0^{(0)}$ has been adjusted to reproduce the $J^{\pi}=18^+$ resonance at an energy $E_{c.m.}=26.5$ MeV suggested by data from the $^{16}O(^{16}O, ^{12}C)^{20}Ne$ reaction.[28] In this figure the nuclear range parameter r_0 of Eq. (2·1) is assumed to be 1.25 fm. In the same way as in the ^{12}C-^{12}C system, the aligned rotational bands come close to the elastic molecular band and almost all of them cross it at spins $16\sim22\,\hbar$. The spin values of the crossings are larger than those of the ^{12}C-^{12}C system, due to the different excitation energies, intrinsic spin and moment of inertia. The inelastic molecular bands (open circles, triangles and squares) include the excitation of the clustering states whose resonance positions may be shifted to lower energies for the same reason as in the case of the 0_2^+ channel of $^{12}C+^{12}C$ (see § 4.1).

In Fig. 9 we can see that the aligned molecular bands with the single

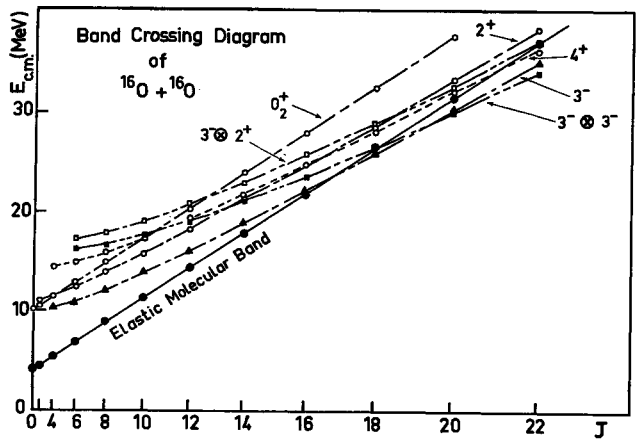

Fig. 9. Band crossing diagram of the $^{16}O+^{16}O$ system. Definitions of the symbols are the same as in Fig. 6. Open symbols refer to an inclusion of cluster state excitations, which implies a possible shift in energies.

and the mutual excitations of the 3_1^- states cross the elastic molecular band at energies 20~30 MeV with spins 16~18 $\hbar$, where the unexcited ions in the entrance channel can couple readily to exit channels in which one or both of the ions are left in the 3^- state, i.e., to inelastic exit channels. This schematic discussion can explain the systematic structure observed in the gamma-radiation data.[17]

In order to examine the relevance of the model to the resonances observed in the gamma-radiation data, we will investigate a consistent explanation of all the available data on the energy dependence of the $^{16}O+^{16}O$ scattering, i.e., elastic scattering,[29] inelastic scattering to the 3_1^- excitation[17] and the fusion cross sections.[30),17] We have carried through a coupled-channel calculation for the ^{16}O-^{16}O system, including the elastic and the aligned 3_1^- inelastic channels. For the moment we do not include the mutual excitation of the 3_1^- state, although the BCM suggests the importance of this channel in the high energy region. The interaction parameters used are listed in Table II. The coupling strengths have been adjusted to reproduce the peak-to-valley ratios in the observed excitation function for total gamma-radiation, and the value

Table II. The potential parameters for the $^{16}O+^{16}O$ system. Depths of the attractive potential of the long range part are assumed to be angular momentum dependent as $V_J=V_0+V_1\cdot L(L+1)$. The definitions of the other parameters are the same as in Table I.

Core Part			Attractive Part				Imaginary Part				Coupling
V_{core} (MeV)	R_{core} (fm)	a_{core} (fm)	V_0 (MeV)	V_1 (MeV)	R_0 (fm)	a (fm)	W_0 (MeV)	$\bar{R}$ (fm)	$\bar{Q}$ (MeV)	ΔJ (N.D.)	r_3 (N.D.)
100.0	3.5	0.30	−16.0	−0.014	6.55	0.5	$0.3E_{c.m.}$	6.7	−7.7	0.4	0.13

thus chosen, $\gamma_3 = 0.13$, is in reasonable agreement with that used in a study of the ^{12}C-^{16}O system, $\gamma_3 = 0.1$, which will be given in the next subsection. We emphasize that the angular momentum dependence of the imaginary potential ··· such that the grazing partial waves are weakly absorbed and the lower partial waves are strongly absorbed ··· plays a very important role in our model calculation in reproducing both the widths of characteristic energy dependent structure and the magnitude of the fusion cross section. We will discuss such an angular momentum dependence of the imaginary part in § 5.

In Fig. 10 we compare our calculated 3_1^- inelastic excitation function[14)] with the data[17)] on gamma radiation deexciting the 3_1^- state. The fact that the measured cross sections are larger than those calculated may partly reflect the neglect of the mutual 3_1^- excitation channel whose aligned band also crosses in the energy region as is shown in Fig. 9. In addition there may exist contributions from inelastic scattering to states in ^{16}O higher than 6.13 MeV in excitation, ··· which thereafter deexcite via cascades through that state ··· as well as reactions leading to a $^{12}C+^{20}Ne$ final channel, wherein the excited ^{20}Ne subsequently decays to excited state in ^{16}O which deexcites either in cascade or directly from the 6.13 MeV 3_1^- state. These additional contributions to the 6.13 MeV gamma radiation yield might be expected to increase smoothly as a function of energy as the background in the data seems to behave. What is gratifying, however, is that the locations, widths and peak-to-valley ratios of the structure that appear to be super-imposed on a monotonically increasing background in the experimental data are reproduced rather well by the calculated curve. Furthermore in Fig. 11, we compare our model calculations with

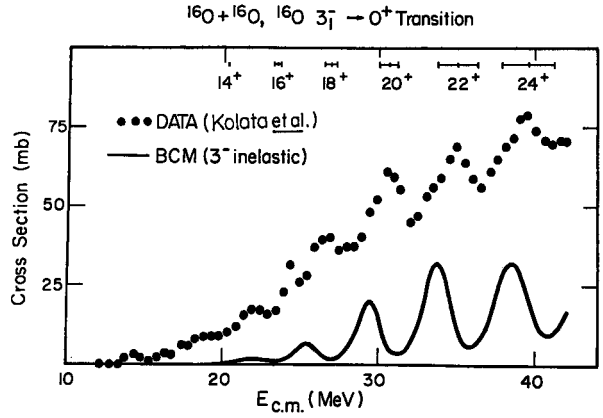

Fig. 10. Inelastic 3_1^- cross section in the $^{16}O+^{16}O$ system. The solid line shows the angle integrated inelastic cross section evaluated by coupled-channel calculations based on the BCM. Data (Ref. 17)) of γ-radiation de-exciting the 3_1^- state of ^{16}O are also indicated. Energies, widths and spins of the zeroth order resonances in the inelastic aligned molecular band are shown in the upper part of the panel.

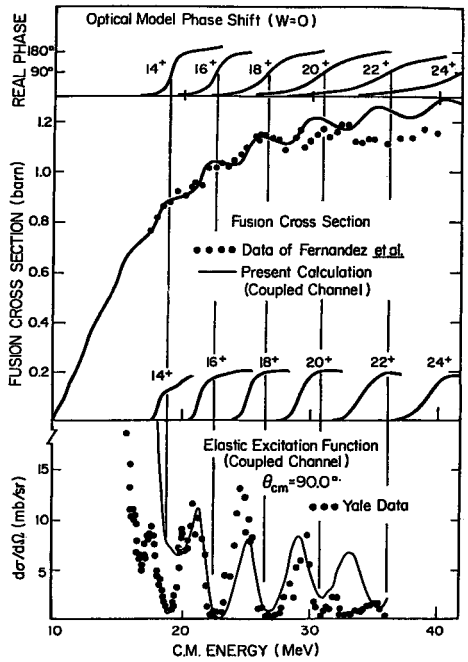

Fig. 11. Fusion cross section and elastic excitation function of the $^{16}O+^{16}O$ system. The middle and lower panels show the comparison between the results and experimental data for the fusion cross section (Ref. 30a)) and the elastic excitation function at $\theta_{c.m.}=90°$ (Ref. 29)), respectively. In the upper panel, real phase shifts of the elastic scattering without absorption are shown.

one of the observed fusion data[30a)] and the data[29)] on the 90° elastic scattering excitation function. Obviously we again obtain gratifying agreement for both of them. In the center of the figure we also show the calculated contribution to the fusion cross section from each identified partial wave. The structure in the fusion cross section can be identified readily with the contribution resulting from each new partial weve as it becomes active with increasing energy. At the top of the figure we show the energy dependence of the phase shifts of the elastic channel for the potential without the imaginary part and without taking into account the coupling with the inelastic channel. The resonance energy of each grazing partial wave, where the phase shift becomes 90° and has a positive slope, corresponds to the peak of each partial fusion cross section. Thus each oscillation of the observed fusion cross section could be interpreted as a reflection of shape resonances of the grazing partial waves in the entrance channel. A discussion about the origin of the oscillation will be given further in § 5. The prediction of this model for the observed elastic excitation functions for all 5 different angles[29)] are as good as that shown here for 90°. In the past the maxima in the 90° elastic excitation function were accepted as resonances.[10b)] As our model calculation shows, when all the above-mentioned data, i.e., inelastic, fusion and elastic data, are considered simultaneously, it is strongly suggested that the minima in the 90° elastic excitation function actually correspond to the resonances and reflect destructive interference between the resonant and the background elastic amplitudes. This

naturally explains the anti-correlation between the fusion and the elastic scattering excitation functions first noted by Kolata et al.[31] Another interesting point is that our model does not reproduce the fragmentation of the gross maxima in the elastic excitation function obtained by Scheid et al.[9] which is also apparent in the experimental data. This difference may reflect our use of the same imaginary potential in both elastic and inelastic channels (see Eq. (3·11)), whereas Scheid et al. used a substantially weaker imaginary potential in the inelastic channel. It should be noticed that the width of the intermediate structure in the elastic scattering is typically about 300 keV, while the characteristic width of the observed structure of the gamma radiation data is 1∼3 MeV. This may suggest different origins for these structures. It would be interesting to learn whether the gamma radiation yield data show structure of few hundred keV characteristic width or not.

We have checked the possible influence of channels other than the aligned one by comparing these results with those obtained in the full space of the 3_1^- excitation. We found no meaningful difference between two calculations for the above results, which justifies the truncation of the model space suggested by the BCM.

To summarize the present analysis suggests that the fusion structure reflects shape resonances of the grazing partial waves in the entrance channel while the structure of the inelastic cross section reflects resonant mixing of waves functions between the elastic molecular band and the inelastic aligned one. One of the major questions in the study of the molecular resonance phenomena was that there was no apparent evidence for molecular states in the ^{16}O-^{16}O system. Now, some resonances have been found at energies well above the Coulomb barrier, just as predicted by the BCM. So the lack of the resonance phenomena in the total reaction cross section near the Coulomb barrier reflects not the absence of the molecular structure but rather that they are marked by a great many competing non-resonant amplitudes as noted by Hanson et al.[32]

4.3. ^{12}C-^{16}O *scattering*

A band crossing diagram of this system is shown in Fig. 12, which includes the 2_1^+ (4.44 MeV) state of ^{12}C and the 3_1^- (6.13 MeV) state of ^{16}O as well as excitations of their α-clustering states. The elastic molecular band is fixed so that for the range parameter $r_0 = 1.25$ fm the 14^+ resonance coincides in energy with the 19.7 MeV resonance which has been seen in the elastic scattering and has been reliably considered 14^+ [16a] We simply assume in Fig. 12 that the molecular band has no parity dependence, although a parity dependence at least for low spins in non-identical heavy-ion systems has been demonstrated by a microscopic calculation.[13] Such a possibility is indicated by arrows in Fig. 12. We expect effects due to the parity dependence to be small at the high spins under consideration. Open circles, triangles and

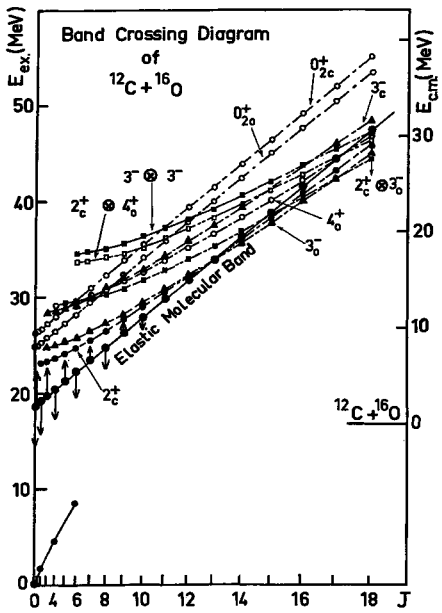

Fig. 12. Band crossing diagram of the $^{12}C+^{16}O$ system. Definitions of symbols are the same as in Figs. 6 and 9. Subscripts C and O indicate Carbon and Oxygen nuclei, respectively. Arrows attached to the elastic molecular band imply a possible parity dependence in the low spin members as shown in Ref. 14), which may cause shifts also in the excited molecular bands.

squares include excitations of α-clustering states, so that the energy positions might shift due to possible changes of the interactions between nuclei as has been mentioned in § 4.1.

The aligned bands of the excitations of 2_1^+ (4.44 MeV) state and the 3_1^- (6.13 MeV) state and of their mutual excitation cross the elastic molecular band and cross with each other at high spins. Thus we can expect molecular resonances with collective excitations as their dominant components at spins $11\hbar$ to $17\hbar$. Further the excitation of the 3_1^- (9.64 MeV) state of ^{12}C and the mutual excitation of the 3_1^- (9.64 MeV) state of ^{12}C and the 3_1^- (6.13 MeV) state of ^{16}O will appear as dominant components of resonances at spins equal to $17\hbar \sim 18\hbar$. It is interesting to note that the aligned bands built on the 4_1^+ (10.35 MeV) state of ^{16}O and the mutual excitations of the 4_1^+ (10.35 MeV) state of ^{16}O and the 2_1^+ (4.44 MeV) state of ^{12}C cross the elastic molecular band at a spin of about $17\hbar$. Another 4_2^+ (11.10 MeV) state of ^{16}O and the 4_1^+ (14.08 MeV) state of ^{12}C will also play an important role at little higher spins and hence at higher energies. These situations are consistent with recent measurements at Tsukuba.[16d)]

Since the discovery of the resonance at 19.7 MeV with spin $14\hbar$,[16a)] there have been several reports of the existence of resonances with so-called "intermediate width". These were summarized by Schiffer[33)] who suggested the possible existence of a rotational or a quasi-rotational band at high excitation energies of ^{28}Si. Our first comment[14a,b)] about the importance of the role of an aligned rotational band was made in order to explain the above-mentioned experimental data, including resonance features clearly observed in the elastic

excitation function of ^{12}C-^{16}O scattering at backward angles.[34] At that time new experimental data appeared on the systematic existence of resonances in this system. Malmin and Paul[35] have observed a series of doublet-like resonances in the inelastic excitation functions to the $^{16}O^*(0_2^+, 3^-; 6.1\,\text{MeV})$, the $^{12}C^*(2^+, 4.44\,\text{MeV})$ and to some other excited states. It is certainly expected from Fig. 12 that such a fragmentation would be produced by an interplay of the elastic and the aligned molecular band in the same energy region as that of the experiments.

First we have performed a coupled-channel calculation by introducing the coupling of the elastic channel with only the $^{16}O^*(3^-, 6.13\,\text{MeV})$, in order to see how the fragmentation will occur due to the band crossing. The potential parameters used are listed in Table III. The essential assumption is in setting up a potential resonance with spin $14\,\hbar$ in the elastic channel at an energy of about 20 MeV, which is strongly suggested by the experiment of Malmin et al.[16a] The depth of the potential in the inelastic channel is slightly changed so as to reproduce the doublet-like resonances close to the experimental energies. Energies and widths of the potential resonances (without an imaginary potential) have been calculated and are listed in Table IV. The resonance energies and barrier heights are plotted in Fig. 13. We can see that the

Table III. The potential parameters for the $^{12}C+^{16}O$ system. Functional form of the short range repulsive soft core is assumed to be Gaussian as $V_G \cdot \exp(-gr^2)$. The definitions of the other parameters are the same as in Table I, although V_2 and V_3 are the depths for the 2_1^+ and 3_1^- inelastic channels.

Core Part		Attractive Part					Imaginary Part				Coupling	
V_G (MeV)	g (fm^{-2})	V_1 (MeV)	V_2 (MeV)	V_3 (MeV)	R_0 (fm)	a (fm)	W_0 (MeV)	$\bar{R}$ (fm)	$\bar{Q}$ (MeV)	ΔJ (N.D.)	β_2 (N.D.)	γ_3 (N.D.)
100.0	0.156	−24.0	−22.0	−22.0	6.01	0.4	−1.0	6.01	−8.0	0.5	−0.1	0.1

Table IV. Calculated energies and widths of potential resonances in the $^{12}C+^{16}O$ system. a) and b) are for the case of the depth parameter $V=-24.0$ MeV and $V=-22.0$ MeV, respectively. In this case the imaginary part is neglected and the other parameters used are the same as in Table III.

a)

J^π	10^+	11^-	12^+	13^-	14^+	15^-	16^+	17^-
E_r (MeV)	10.14	12.43	14.84	17.35	19.98	22.74	25.65	28.75
$\Gamma_{s.p.}$ (MeV)	0.0012	0.012	0.065	0.20	0.46	0.98	1.45	2.26

b)

J^π	10^+	11^-	12^+	13^-	14^+	15^-	16^+	17^-
E_r (MeV)	11.55	13.76	16.08	18.52	21.10	23.86	26.80	29.96
$\Gamma_{s.p.}$ (MeV)	0.016	0.071	0.22	0.49	0.78	1.45	2.37	3.51

aligned molecular band crosses the elastic one at spin 14^+ and that the curve of the barrier heights for the aligned inelastic channel crosses that for the elastic channel at a spin about 17^-. As was discussed in § 2, the latter means that the potential resonance widths in the aligned band are smaller than those in the elastic band for spins lower than $17\,\hbar$, if the resonance energies are close to each other. In the bottom panel of Fig. 14, the calculated excitation function of the inelastic scattering to the $^{16}O^*(3^-, 6.13\,\mathrm{MeV})$ is shown, where

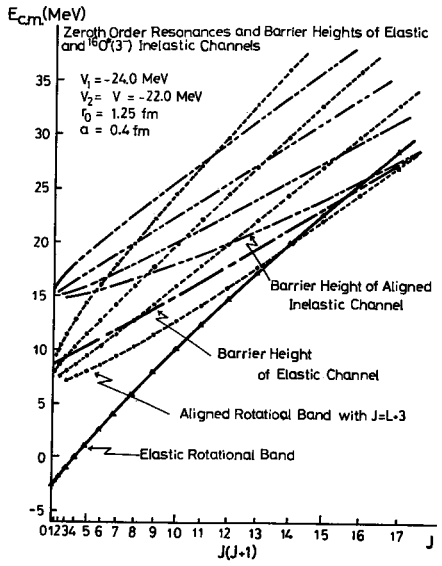

Fig. 13. Resonances in the zeroth order and barrier heights of the elastic and $^{16}O^*$ $(3^-, 6.13\,\mathrm{MeV})$ inelastic channels in the $^{12}C+^{16}O$ system. Potential parameters adopted are given in Table III.

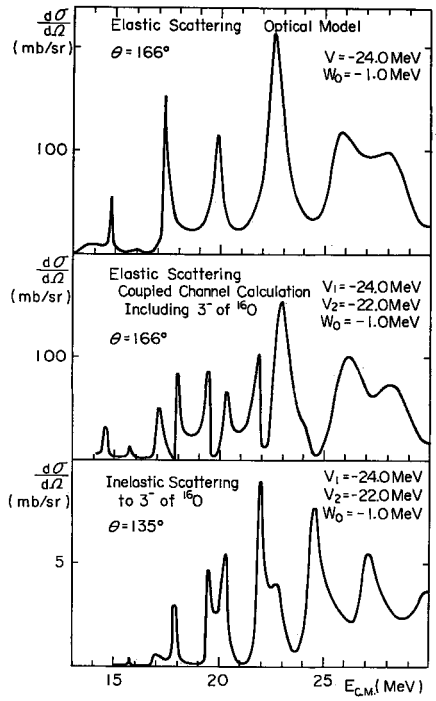

Fig. 14. Fragmentation of resonances due to a band crossing between the elastic and the inelastic molecular bands in the case of $^{12}C+^{16}O$ scattering with $^{16}O^*$ $(3^-, 6.13\,\mathrm{MeV})$ excitation. Calculated excitation functions of the elastic and inelastic scattering are shown at the middle and the bottom, respectively, where the elastic and $^{16}O^*$ $(3^-, 6.13\,\mathrm{MeV})$ inelastic channels are included in the model space. In the upper panel calculated elastic excitation function is shown in which only the elastic channel is involved, for the purpose of comparison. Adopted parameters are given in Table III.

the coupling strength γ_3 is taken to be 0.1. We can see that our model reproduces the doublet-like resonances observed in the inelastic excitation function. The calculated elastic excitation function is shown in the middle panel of Fig. 14. We can see that it has intermediate structures which originate from the fragmentation of potential resonances due to the band crossing. We can readily recognize it by comparing the excitation functions calculated by the optical model shown in the top panel of Fig. 14 and by the coupled-channel calculation shown in the middle panel of Fig. 14. Each resonance peak in the former splits into two peaks in the latter. The dominance of the aligned configuration in these resonances, which is one of the characteristic predictions of the BCM, can be seen in the mixing ratios of resonance wave functions. They are calculated in the bound state approximation and are shown in Table V. We can see that at the crossing point (spin equal to 14^+ in this case) the mixing ratio is about half and half between the elastic and aligned molecular bands, while apart from the point the mixings become small. The mixings with non-aligned bands are always negligibly small and are omitted from the table. These tendencies just correspond to the band crossing diagram of Figs. 4 and 12. We can thus understand the onset and the fading-away of resonances by the BCM.

Next we have performed a coupled-channel calculation including both the $^{16}O(3^-, 6.13\,MeV)$ and the $^{12}C(2^+, 4.44\,MeV)$ inelastic channels. In the top panel of Fig. 16, the calculated elastic excitation function is shown, which

Table V. Energy eigenvalues and probabilities (mixing ratio) of the resonances in the bound state approximation. The potential parameters used are those in Table III, and the imaginary part is neglected. This result only includes the mixing ratios for the members of the elastic and aligned bands, because the others are negligibly small although the other bands with the 3_1^- excitation are included in the calculation.

J^π	$E_{c.m.}^{BSA}$ (MeV)	elastic	3^--inelastic ($L=J-3$)
12^+	14.70	0.86	0.13
	15.75	0.13	0.86
13^-	17.14	0.70	0.30
	17.95	0.30	0.70
14^+	19.59	0.47	0.53
	20.35	0.53	0.47
15^-	22.05	0.28	0.72
	22.91	0.71	0.28
16^+	24.55	0.18	0.82
	25.52	0.81	0.18

apparently has more structures compared with that shown in the middle panel of Fig. 14 and is closer to the experimental data. The calculated excitation functions of the inelastic scattering to the $^{12}C^*(2^+, 4.44\,MeV)$ and to the $^{16}O^*(3^-, 6.13\,MeV)$ states are shown in the bottom and the middle panels of Fig. 15, respectively. When we proposed the BCM and investigated ^{12}C-^{16}O scattering, we predicted the existence of more resonance peaks in the inelastic excitation functions at energies higher than experimentally observed at that time. It is gratifying that the prediction has been confirmed by recent experiments.[16c,d] It should be mentioned here that the aligned band of the mutual $(2^+, 3^-)$ excitation channel will also play a role in the region

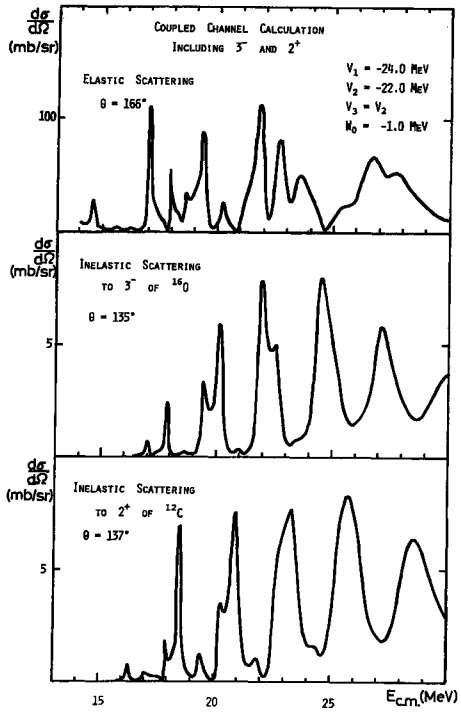

Fig. 15. The calculated excitation function of the elastic, the $^{16}O^*$ $(3^-, 6.13\,MeV)$ and the $^{12}C^*(2^+, 4.44\,MeV)$ inelastic scattering of the $^{12}C+^{16}O$ system. Adopted potential parameters are given in Table III.

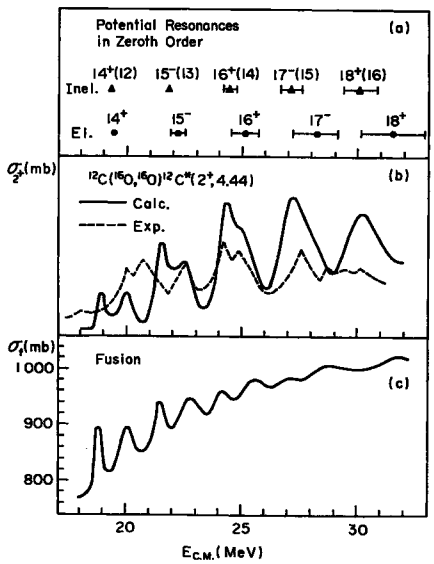

Fig. 16. Comparison of the BCM calculation of the integrated excitation function of $^{12}C^*$ $(2^+, 4.44\,MeV)$ inelastic scattering with the experimental data. (a) The zeroth order energies of potential resonances in the elastic and the inelastic aligned molecular band. The horizontal bars show the widths of the potential resonances without imaginary potential. Numbers in the parentheses indicate the orbital angular momenta between nuclei. (b) The excitation function for the integrated cross section of the $^{12}C^*(2^+, 4.44\,MeV)$ inelastic scattering. The solid line is calculated and the dashed line is experimental (Ref. 16b)). (c) Calculated fusion cross section. The adopted values of the parameters are given in Table VI.

considered, because it crosses the elastic band and the other aligned band there as shown in Fig. 12.

Recently there has been a new wave of activity in the experimental study of heavy-ion resonance reactions. Some of them are measurements of resonances in inelastic channels, especially to the collective excitations, and others of oscillations in fusion reactions. Not only the ^{12}C-^{12}C and ^{16}O-^{16}O systems but also the ^{12}C-^{16}O system has been extensively investigated. The angle integrated excitation functions of the inelastic scattering to the ^{12}C*$(2^+, 4.44\,\mathrm{MeV})$ and ^{16}O*$(3^-, 6.13\,\mathrm{MeV})$ states have also been measured.[15b,f] We can clearly see the existence of resonances in both channels. We have calculated the excitation function to the ^{12}C*$(2^+, 4.44\,\mathrm{MeV})$ inelastic scattering in order to compare the results with the new experimental data. Figure 16 shows preliminary results of our calculation together with the experiment. In this calculation we include only the ^{12}C*$(2^+, 4.44\,\mathrm{MeV})$ inelastic channel. The inclusion of the ^{16}O*$(3^-, 6.13\,\mathrm{MeV})$ channel will not destroy the characteristic features, but will shift the resonance positions slightly and affect the yields a little (see the previous results). The parameters used are listed in Table VI. It is clearly seen in the middle panel of Fig. 16 that the energies, widths and yields of the observed resonances are well reproduced by our simple model. The spin sequence is predicted in the top panel of Fig. 16, where the resonance energies and the widths are also shown in the zeroth order. The calculated fusion cross section is shown in the bottom panel of Fig. 16. They show structure correlating with resonances in the inelastic channel and with those in the elastic channel at higher energies.

Table VI. The potential parameters used in the calculation of ^{12}C(^{16}O, ^{16}O) ^{12}C*$(2_1^+, 4.44\,\mathrm{MeV})$ inelastic scattering. Several values of the parameters are slightly changed from those in Table III for the purpose of better reproduction of the integrated cross section, but the definitions are the same as in Table III.

Core Part		Attractive Part				Imaginary Part				Coupling
V_0 (MeV)	g (fm^{-3})	V_1 (MeV)	V_2 (MeV)	R_0 (fm)	a (fm)	W_0 (MeV)	$\bar{R}$ (fm)	$\bar{Q}$ (MeV)	ΔJ (N.D.)	β_2 (N.D.)
100.0	0.156	−25.0	−24.0	6.01	0.4	−6.0	6.01	−8.0	0.7	0.15

4.4. *Summary of the results*

Several years ago the present authors[14] proposed the BCM in order to explain anomalies observed in the excitation functions of the elastic and the inelastic scattering of the ^{12}C-^{16}O system. The number of the observed resonance-like peaks was larger than that expected from potential resonances in the entrance channel. This seemed to suggest that other degrees of freedom take part in the phenomena. In this connection, the present authors have investigated the consequence of the coupling to collective excited states of heavy-

ions which have been known to couple most strongly to the elastic channel. As shown in Fig. 12, we can draw a band crossing diagram for the system without any artificial assumptions and predict the existence of a region where potential resonances in the inelastic channels will strongly couple to resonances in the elastic channel and will cause fragmentation of resonance strengths of the incident channel. Such regions exist also in the ^{12}C-^{12}C and ^{16}O-^{16}O systems as is shown in Figs. 6 and 9, and probably in some other systems as well.

In order to see whether such a picture can really explain the observed resonance phenomena, coupled-channel calculations have been performed for the above three systems, where resonances are most prominently observed, and the results have been compared with the data. As is shown in the preceding subsections all the resonant excitation functions in the inelastic scattering to the collective levels of heavy-ions have been found to be systematically reproduced. In the present calculations we have used simple optical potentials, whose real parts have been set to have a rotational series of potential resonances according to the band crossing diagram and whose imaginary parts have been assumed phenomenologically to be J-dependent so as to guarantee "surface transparency". We have not assumed any channel-dependent imaginary potential which is often used by other authors so as to easily reproduce rather sharp resonances, because we have no explicit reason for this yet. The physical origin of the surface transparency will be discussed in the next section in the light of recent developments in understanding the mechanism of fusion reaction. As for the real part of the optical potential, several authors[20] have claimed from results of the folding calculations that the coupling to collective excitations is much stronger than that used in the present macroscopic model. We should be careful in drawing a conclusion about the coupling strength from the calculations using folding model, because the folding potential does not take into account the Pauli exchange effects, which have been found to be very important in microscopic studies (see Chapter V). Anyhow, although there are some quantitative differences, coupled channel calculations with folding potentials have been found to give resonance excitation functions similar to those given in the present work and have also confirmed the importance of aligned configurations.

It is, of course, necessary to make refined calculation with more realistic optical potential and taking into account more of the inelastic channels which are expected to be important from the band crossing diagrams (Figs. 6, 9 and 12). It is also necessary to analyse angular distributions in order to confirm the validity of our model. At the same time more experimental information on the spin values of resonances is strongly desirable. At present there is only one widely accepted spin assignment, i.e., the 14^+ resonance at 19.7 MeV[16a] in the case of the $^{12}C+^{16}O$ system, although several spin assignments which give different spin values for the doublet-like resonances have been

reported.[16g,h] Systematic measurements of integrated excitation functions in various inelastic channels are also desirable, especially for the $^{16}O+^{16}O$ system. Such data will enable the partial width distributions to be determined.

To summarize, the BCM can predict the existence of region where fragmentations of resonance strengths due to coupling to the collective sates of heavy-ions occur to generate intermediate structures and it can quantitatively explain the resonances observed systematically in the inelastic scattering excitation functions. In other words, the BCM provides a simple plausible base, from which we can refine our investigations and will reach a profounder understanding of resonance mechanisms in heavy-ion reactions and of nuclear structures of resonance states in the high excitation region of the compound system.

Before proceeding to the next section, we emphasize again the importance of aligned molecular bands, which are predicted to dominate in prominent resonances. This means that resonances have special orientations of the intrinsic spin and the orbital angular momentum between two heavy-ions. Such special structures will be observed by polarization type experiments, for example, by measurement of magnetic sub-state populations.[36]

One of the important implications of the BCM is that in order to observe prominent resonances the potential resonances in the two channels should be close to each other. If there is a potential resonance in a rearrangement channel and if it is close to a potential resonance with the same spin in the incident channel, one can expect to clearly observe a resonance in the exit rearrangement channel such as α and ^{8}Be channels. This point will be discussed in § 6.

§ 5. The fusion cross section in light heavy-ion reactions and the imaginary part of the interaction potential

In the analyses of resonances by the BCM, we have employed the phenomenological potentials between nuclei. The imaginary part is assumed to have a J-dependence[10b] so as to guarantee the "surface transparency", the existence of which has been demonstrated in optical model analyses of heavy-ion elastic scattering.[10] In the present calculations on the ^{12}C-^{12}C, ^{12}C-^{16}O and ^{16}O-^{16}O systems at energies well above the Coulomb barrier, we have always chosen the values of the parameters so that the critical angular momentum, J_c in Eq. (3·12) is nearly equal to or smaller than the grazing angular momentum J_g which is obtained from Eq. (2·2) with $B_{J=L}{}^{(0)}$ equal to $E_{\text{c.m.}}$. This means that the grazing partial wave feels weak absorption and its potential resonance can survive with an observable width in the energy region. Although the surface transparency is quite important, little theoretical explanation for it has been given. What we can do at present is to justify it qualitatively, based on the recent development in understanding the mechanism of fusion.

In this section we first introduce the recent phenomenological study of the fusion cross section in the light heavy-ion reactions which has been performed by Lee, Arima and one of the present authors (T.M.).[11a] Next we will discuss the surface-transparent character of heavy-ion optical potentials in connection with the fusion reaction mechanism. Finally we will make a new attempt to understand consistently resonance phenomena and fusion reactions, although we do not yet have a practical method to treat resonant channels and all the other possible reaction channels on the same footing.

5.1. *Phenomenological study of the fusion cross section in light heavy-ion reactions*

As is well known, the excitation function of the fusion cross section in light heavy-ion reactions ($A<80$, A means the mass number of the compound nucleus) shows a bending at a certain energy.[37] At energies lower than the bending energy, the fusion cross section is almost equal to the total reaction cross section and at higher energies it is smaller than the total reaction cross section. In experiments, almost all the observed fusion cross sections are determined by the evaporation residues in the light heavy-ion reactions. It is then expected that the observed fusion cross sections are closely related to the compound nucleus formation in the reaction process.

To investigate phenomenologically the character of the fusion cross section, the angular momentum sharp cutoff model is usually used. In the sharp cutoff model the fusion cross section σ_f is given by the following formula for spinless systems:

$$\sigma_f=\frac{\pi}{k^2}\sum_{L=0}^{L_{cr}}(2L+1)=\frac{\pi}{k^2}(L_{cr}+1)^2, \tag{5·1}$$

where k is the wave number of the entrance channel, and L_{cr} is the critical angular momentum which limits the angular momentum contributing to the fusion at the given energy. As is expected from the energy dependence of the fusion cross section in the energy region below the bending energy, the critical angular momentum L_{cr} is determined reasonably well by the penetration of the barrier which is composed mainly of the Coulomb and centrifugal barriers at the contact distance region. As already shown in § 2, the barrier height is simply represented as follows,

$$V_B(L)=V_B(R_B)+\frac{\hbar^2}{2\mu R_B^2}L(L+1), \tag{5·2}$$

where $V_B(R_B)$ is the barrier height for S-wave, i.e., roughly equal to the Coulomb barrier, R_B is the relative distance corresponding to the top of the barrier, and μ is the reduced mass of the entrance system. To evaluate the critical angular momentum L_{cr} for the energies higher than the bending energy, the critical distance model has been proposed by several authors.[38] An es

sential assumption in the model is the existence of the fusion barrier $V_{cr}(L)$ at the critical distance R_{cr} smaller than the radius R_B of Eq. (5·2),

$$V_{cr}(L)=V_{cr}+\frac{\hbar^2}{2\mu R_{cr}^2}L(L+1), \tag{5·3}$$

where the parameter V_{cr} is the fusion barrier for S-wave. By the use of the Eqs. (5·2) and (5·3), the fusion cross section is written by the following formulae,

$$\sigma_f \cong \pi R_B^2\left(1-\frac{V_B}{E_{c.m.}}\right); \text{ for lower energy region,} \tag{5·4}$$

$$\sigma_f \cong \pi R_{cr}^2\left(1-\frac{V_{cr}}{E_{c.m.}}\right); \text{ for higher energy region.} \tag{5·5}$$

As is well known, Glas and Mosel[39] have succeeded in combining these two formulae by using a simple formulation. Many observed fusion cross sections have been analysed by the use of the critical distance model. We have however, no clear physical insight of the model up to now.

On the other hand, an alternative way of considering the critical angular momentum L_{cr} which has been discussed for some time is that the fusion cross section might be limited by the yrast line L_y of the compound nucleus, namely $L_{cr}=L_y$.[40] In order to justify the critical distance model, Glas and Mosel[41] have, however, shown that the experimentally determined L_{cr} values are always smaller than the calculated values for the yrast states. This could be taken to disprove the yrast limitation. On the other hand this has been discussed by Lee et al.[11a] and shown to be very reasonable.

In a naive sense, it is natural to consider that two heavy-ions do not fuse at the yrast line of the compound nucleus, because here the nuclear level density is very low. However they can fuse at the energy region somewhat above the yrast line, in which the level density is expected to be high enough, i.e., the nuclear temperature is high. Lee et al. have thus proposed the concept of the "statistical yrast line L_y^{st}" of a compound nucleus, which determines the critical angular momentum L_{cr}. The energy of the statistical yrast line $E_{y,st}^*$ is assumed to run nearly parallel to the usual yrast line with additional energy ΔQ,

$$\begin{aligned} E_{y,st}^* &= \frac{\hbar^2}{2\mathcal{J}_c}L_y^{st}\cdot(L_y^{st}+1)+\Delta Q, \\ &= \frac{\hbar^2}{2\mathcal{J}_c}L_{cr}\cdot(L_{cr}+1)+\Delta Q, \end{aligned} \tag{5·6}$$

where $\mathcal{J}_c$ is the moment of inertia of the compound nucleus A and is assumed to be equal to that of a rigid body for simplicity, $\mathcal{J}_c=\mathcal{J}_{rig}=2/5\cdot M\cdot A\cdot R^2$ and

$R=r_{0f}A^{1/3}$. The excitation energy of the compound nucleus E^* is the sum $E_{\text{c.m.}}+Q$, where Q is the Q-value of the entrance system. From Eqs. (5·1) and (5·6), the fusion cross section in the energy region above the bending energy becomes as follows,

$$\sigma_f \simeq \frac{\pi \mathcal{J}_c}{\mu}\left(1+\frac{Q-\Delta Q}{E_{\text{c.m.}}}\right). \tag{5·7}$$

This expression contains two parameters ΔQ and r_{0f} which are properties of the compound nucleus. On the other hand the entrance channel determines the values of Q and μ. It is obvious that the slope of the fusion cross section depends on the value of $\pi \mathcal{J}_c/\mu(Q-\Delta Q)$. Then if the systematic values of r_{0f} and ΔQ in Eq. (5·7) are found, Eq. (5·7) can predict the values of the fusion cross section in the energy region above the bending energy.

In order to obtain systematic values for ΔQ and r_{0f}, Lee et al. have analysed the observed fusion cross sections of the several systems such as ^{16}O-^{40}Ca and ^{32}S-^{24}Mg,[37] and have found the values $r_{0f}=1.20\pm0.05$ fm and $\Delta Q=10.0\pm2.5$ MeV. It should be stressed that the value for ΔQ is consistent with the energy region at which the level density of the compound nucleus is high. In order to show the validity of this model, the fusion cross section at the observed bending energy calculated by the use of Eq. (5·7) is shown in Fig. 17 and is compared with the experimental value for several systems. This figure shows that the observed fusion cross sections are reproduced well by Eq. (5·7) and that the variation of the values from system to system can be understood as just a manifestation of the Q-

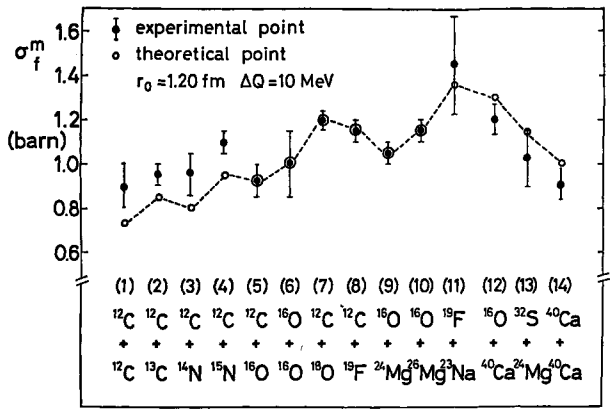

Fig. 17. Closed circles are the measured values of the fusion cross section for various systems at the observed bending energy. The data were mostly taken from the original papers cited in Refs. 37), 38) and 42) except for reaction (4) which was taken from Ref. 62). and for reaction (11) from Ref. 63). Open circles are the values calculated at the same energy by use of Eq. (5·7) with $r_{0f}=1.20$ fm and $\Delta Q=10.0$ MeV. The dashed line is a guide for the eyes.

value effect. These observed variations in the fusion cross section have been explained as the effect of valence nucleons on the critical distance in Eq. (5·5).[42]

A theoretical interpretation of the physical meaning of ΔQ, namely the physical basis of the statistical yrast line, has been shown by Arima, Lee and one of the present authors (T.M.).[11a] The essence of their study is as follows. Adopting the scattering theory by Mahaux and Weidenmüller[43] for the averaged scattering amplitude of the entrance channel they have obtained the following scattering amplitude S_J which includes the coupling between the entrance channel and complicated compound states,

$$S_J = e^{2i\delta_J}[(1-P_J(E_{\text{c.m.}})) + P_J(E_{\text{c.m.}})\, e^{-\pi\rho_J(E^*)\Gamma_J}], \tag{5·8}$$

where δ_J is a real phase shift without coupling to the compound states and $P_J(E_{\text{c.m.}})$ is the penetration factor of the potential barrier at the contact region. $\rho_J(E^*)$ is the level density of the compound nucleus and Γ_J are the partial widths which come from the coupling between the entrance channel and the compound states. The partial widths Γ_J are estimated by using the results of the microscopic study between composite nuclei.[44] From Eq. (5·8), strong absorption can be expected in the energy region where the values $\pi\rho_J(E^*)\Gamma_J$ become large, i.e., $\pi\rho_J(E^*)\Gamma_J \gg 1$. They have found that the transmission coefficients $T_J = 1-|S_J|^2$ for compound nucleus formation become nearly 0.5 for almost all systems ($A<80$) at $\Delta Q \simeq 10$ MeV above the usual yrast line.

It is hoped that these quantities obtained above are represented by the imaginary potential of the interactions between composite nuclei. However it is rather difficult to construct the potential because we have no clear information about the spatial part of the potential up to now.

5.2. *Consideration of the imaginary part of the interaction potential*

It is important to note that for the fusion cross section at high energies there exsists a critical angular momentum smaller than grazing. The arguments in § 5.1 strongly suggest that the critical angular momentum is determined by the statistical character of the compound nucleus. Based on this explanation, we propose a simple picture of the energy- and angular momentum-dependences of the imaginary potential. The critical angular momentum J_{cf} for strong absorption due to compound nucleus formation is estimated from Eq. (5·6),

$$J_{cf} \simeq \sqrt{\frac{2\mathcal{J}_c}{\hbar^2}(E_{\text{c.m.}} + Q - \Delta Q)}. \tag{5·9}$$

This expression turns into Eq. (3·12), if we replace $\mathcal{J}_c$ by $\mu\cdot\bar{R}^2$ and $Q-\Delta Q$ by $\bar{Q}$. The physical meaning of this J_{cf} is, however, completely different from that given by Chatwin et al.[10b] They discussed that the J-dependence should

come from a matching to outgoing channels which could carry away angular momenta brought in by the entrance channel. Such a mechanism would be effective and dominate at much higher energies than the bending energy. At slightly higher energies than the bending energy the effective direct reaction channels are only the inelastic ones in the systems considered in this chapter. This situation is clearly seen in an energy dependence of the number of open channels with a spin corresponding to the grazing partial wave, which will be given elsewhere.[45] Thus the imaginary potential which is used in coupled-channel calculations should have a characteristic spin- and/or energy-dependence determined by fusion reaction. In actual calculations we have used the parametrization of Eq. (3·12). Figure 18 shows the energy-dependences of J_c given by Eq. (3·12), J_{cf} given by Eq. (5·9) and J_g which is obtained from Eq. (2·2) by inserting $E_{\text{c.m.}}$ instead of $B_{J=L}{}^{(0)}$, for the ^{12}C-^{12}C system as an example. Apparently the J_c curve does not coincide with the J_{cf} curve. This is not surprising because actual critical angular momenta in the calculation are determined by the combined effect of the J_c and W_0 with an arbitrarily chosen Woods-Saxon form factor of Eq. (3·11). Nevertheless the J_c curve is still indicative of the surface transparency. It is also worth noticing here that at much higher energies than the bending energy we must take into account the effects of direct reactions.

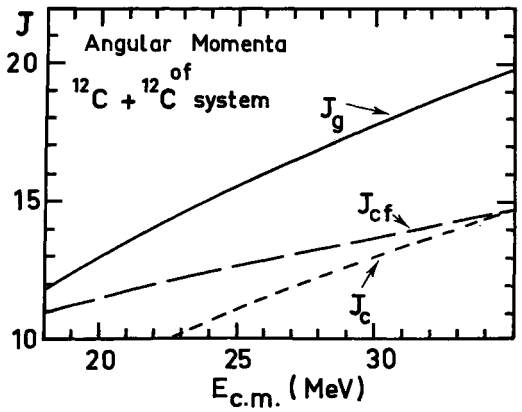

Fig. 18. Energy dependence of the angular momenta, J_g, J_c and J_{cf} for the ^{12}C+^{12}C system (see the text for their definitions). The values of parameters are taken from Table I.

The above argument is one of the possible explanations of the surface transparency of the optical potential in heavy-ion scattering, which is illustrated in Fig. 19. As already mentioned, it is gratifying that the surface transparent region, i.e., the energy near and above the bending energy in the fusion cross section just overlaps with the region where the band crossings occur between the elastic and excited molecular bands. This means that there exists a region of nuclear molecular resonances, where the resonances suffer little from the strong absorption.

We, however, know that resonances are obseved also in the energy region

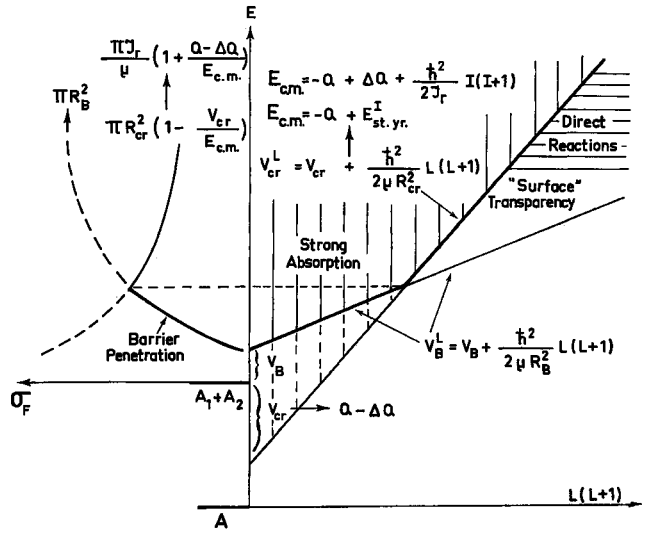

Fig. 19. Schematic explanation of "molecular resonance region" (surface transparency) in relation to the fusion cross section. A possible explanation on bending phenomena in the fusion cross section is also given according to Ref. 11). See the text for details.

below the bending energy in such systems as ^{12}C-^{12}C and ^{12}C-^{16}O, where the fusion reaction is dominating and where the interactions would be expected to be strongly absorptive. A possible explanation is, as has been well known, that the level density of the compound nucleus and the number of open channels are much smaller than those in other systems which do not show any resonances.[32] Anyhow we have not yet obtained a practical expression for the imaginary potential theoretically, which represents an absorption due to fusion reaction and hence contains the characteristic aspects of the reaction dynamics. Another possible approach is to renounce the concept of the imaginary potential and to construct a new theoretical framework where the strong absorption and the resonances would be treated separately. An attempt has been made by Arima et al.[11a] by constructing the averaged scattering amplitude (see Eq. (5·8)). The present authors[40] have also made an attempt to incorporate strong absorption and resonance phenomena without referring to any imaginary potential, and have proposed a new treatment by using the smooth-cut-off model.[47]

5.3. *An attempt to develop a new treatment of heavy-ion scattering*

From the above considerations about the resonance and fusion reaction mechanisms it would seem plausible that they could be treated separately. First we will evaluate the gross energy dependence of the absorption effect on the S-matrix elements and then incorporate it into physical S-matrix ele-

ments which carry the molecular resonances.

In order to obtain the gross energy dependence we must analyse the fusion cross section, because the fusion reaction, except for the resonant inelastic channels, is the dominant reaction channel which carries the incident flux away. First we will estimate the energy dependence of the barrier penetration factor which is expected to play an important role in the fusion reaction, because we consider that the fusion reaction takes place inside rather than outside the barrier. Transmission coefficients are calculated in a semi-classical approximation[48] using an inverted parabolic approximation to the potential shape in the region of the outer barrier. According to this model the transmission coefficient is as follows,

$$T_L=\frac{1}{1+\exp\left[2\pi\left(E_L-E_{\text{c.m.}}\right)/\hbar\omega_L\right]}, \tag{5·10}$$

where E_L is the energy of the barrier top for angular momentum L, and $\hbar\omega_L$ is given as follows,

$$\hbar\omega_L=\hbar\sqrt{\frac{1}{\mu}\left|\frac{d^2V_L}{dr^2}\right|_{r=R_B}}. \tag{5·11}$$

In this expression V_L is the total potential including the centrifugal term adopted in the BCM calculations. Assuming that there is strong absorption somewhere inside the potential barrier, the absorption cross section is calculated by the following expression,

$$\begin{aligned}\sigma_{\text{abs}}(E_{\text{c.m.}}) &=\frac{\pi}{k^2}\sum_L(2L+1)\cdot T_L,\\ &=\frac{\pi}{k^2}\sum_L(2L+1)\cdot(1-\eta_L{}^2).\end{aligned} \tag{5·12}$$

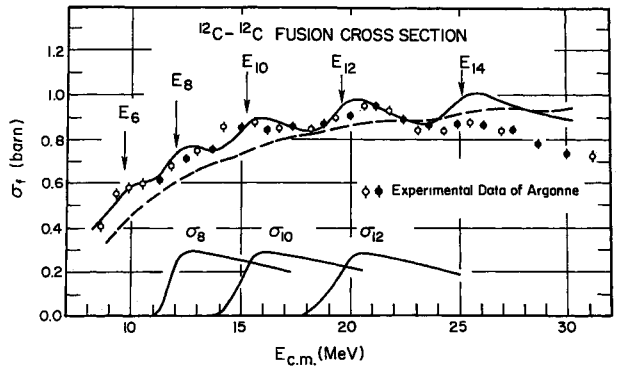

Fig. 20. Analysis of the fusion cross section in the $^{12}C+^{12}C$ system. Solid lines show the results calculated in the smooth-cutoff model. Vertical arrows show the values of E_L. Several partial wave contributions are shown. The dashed line shows the fusion cross section estimated by the semi-classical treatment of the barrier penetration.

The result is shown in Fig. 20 by the dashed line, together with the experimental data,[49] for the $^{12}C+^{12}C$ system. We can see that the barrier penetration effect is not enough to reproduce the experiment, especially the evident oscillatory structure, although the barrier penetration does give rise to slight structure. What we require, therefore, is a mechanism to increase the magnitude of the structure and to correspond more nearly with the data. One possibility is to introduce resonances in the entrance channel, as already exemplified in § 4.2 for the ^{16}O-^{16}O system. Another possible mechanism is to introduce energy dependence of the statistical character of compound nucleus, i.e., of the level density, which is shown schematically in Fig. 19. The exponential increase of the level density around the statistical yrast line would give rise to a sharp energy dependence of the partial fusion cross section. Such a possibility is studied in Ref. 11b).

As we do not completely understand the fusion reaction, especially the origin of the oscillation, we analyse it phenomenologically, using a smooth-cutoff model. We parametrize the reflection coefficient with the usual notation as follows:

$$\eta_L(E_{\text{c.m.}}) = \frac{1}{1+\exp[(E_{\text{c.m.}}-E_L)/\Delta E_L]} . \qquad (5\cdot 13)$$

This parametrization implies that the partial wave with angular momentum L will suffer a strong absorption at energies higher than E_L with ΔE_L providing a smooth variation through the transition region. In this calculation, ΔE_L plays much the same role as does $\hbar\omega_L$ in Eq. (5·10) in that both determine the width of the structure. The value of ΔE_L is taken as 0.5 MeV for all the partial waves, from fitting the measured fusion cross section, whereas $\hbar\omega_L$ is implicit in the model. The results are shown also in Fig. 20 by the solid line. In Fig. 20, we see that the oscillatory features of the data are reproduced extremely well by the model as well as the absolute value of the observed fusion cross section. It is interesting to notice here that each maximum in the fusion cross section reflects the contribution of a single partial wave $\sigma_L = (2\pi/k^2)\,(2L+1)\cdot(1-\eta_L{}^2)$, and several of the individual contributions are also shown in Fig. 20. Thus, it can be considered that the maxima are signatures of enhanced absorption suffered by each partial wave as it enters the region of the critical angular momentum or the region of the potential resonance as the incident energy increases.

An important point in our phenomenological analysis in terms of the smooth-cutoff model is that the angular momentum corresponding to each of the maxima in the fusion cross section can be determined unambiguously. If we change the values of E_L artificially so as to associate a different partial wave from that in Fig. 20 with a particular maximum in the fusion cross section, e.g., a partial wave larger or smaller by two units, then we obtain quite different absolute values for the fusion cross section larger or smaller, by about

300 mb, than the original values which agreed very well with the experimental ones.[49] It is important to emphasize that the suggested analysis of the structure in the fusion cross section in terms of a smooth-cutoff model thus provides precise information on the energy dependence of the absorption for each uniquely identified partial wave, information otherwise difficult to obtain.

After we have obtained the reflection coefficients which have been extracted from the fusion cross section, we calculate the molecular resonances which dominate in the region around the top of the effective potential barrier and below the strong absorption energy or the statistical yrast line. We solve the coupled-channel equations using real interactions only, that is, without introducing any imaginary part, because we have already used the smooth-cutoff model as a representation of the absorption effects. The real nuclear potential parameters are adjusted to yield the elastic potential resonance with $J^\pi=12^+$ at about 20 MeV and the resonance $J^\pi=2^+$ at about 6 MeV. The former is suggested by the detailed analysis of correlated resonances[50] as well as by our analysis of the fusion data just presented. The latter has been obtained in a previous analysis of the fragmented 2^+ resonances in the sub-Coulomb region reported by the present authors.[8] The parameters used are listed in Table VII.

Table VII. The potential parameters used in the new attempt (see the text for the detail). An imaginary part is not necessary in the present calculation. The definitions of the parameters are the same as in Table II. Two values for β_2 are those in the first order and in the second order terms in the expansion of long range potential. Inclusion of the second order terms in our expansion is essential to give the rather large inelastic cross section for the mutual 2_1^+ excitation.

Core Part			Attractive Part				Coupling
V_{core} (MeV)	R_{core} (fm)	a_{core} (fm)	V_0 (MeV)	V_1 (MeV)	R_0 (fm)	a (fm)	β_2 (N.D.)
100.0	4.0	0.35	−48.0	−1/17	4.67	0.5	−0.2, −0.7

We define the physical S-matrix element as the product of the $\bar{S}$-matrix element which is obtained by the BCM calculation using only the real potential and the reflection coefficient η_L which has been obtained from the analysis of the fusion cross section with the smooth-cutoff model,

$$S^J_{cc'}=\sqrt{\eta_{L_c}(E_c)}\cdot\bar{S}^J_{cc'}\cdot\sqrt{\eta_{L_{c'}}(E_{c'})}, \qquad (5\cdot14)$$

where L_c and E_c are the orbital angular momentum and the relative kinetic energy available in channel c. It is important to stress that the problem has been factorized; the $\bar{S}^J_{cc'}$ matrix elements describe only real potential effects while the reflection coefficients η_L describe the absorption effects. For the single channel problem, Eq. (5·14) is similar to Eq. (5·8) in the case of the strong absorption limit where the second term on the right-hand side of

Eq. (5·8) vanishes.

By using the physical S-matrix element $S^J_{cc'}$, we calculate cross sections for the inelastic and the elastic scattering, where prominent structure is observed experimentally. In Fig. 21, the fusion and the inelastic scattering cross sections obtained by the present calculation are compared with the experiments.[15),49)] Agreement is not so good for the inelastic cross sections. This comes from the fact that our parametrized reflection coefficents η_L are forced to approach smoothly zero at higher energies than the E_L (see Eq. (5·13)). The results, however, reproduce qualitatively the fragmentation of the resonances and the resonances appear just before the fusion maxima; this is consistent with our picture. The experimental data also exhibit such differences between the energies of the molecular resonances and the fusion maxima if one looks carefully. A more drastic example is the $^{12}C+^{16}O$ system, where an anti-correlation between resonances in the inelastic scattering and the fusion oscillations has been observed.[51)] This feature seems important for specifying the reaction mechanism between heavy-ions. As is shown semi-quantitatively in Fig. 21, our picture explains this feature: After the incident wave comes into the interaction region beyond the outer potential barrier, various reactions are possible in general, but for some higher partial waves, only the inelastic scattering is effectively possible and then effects of the real potential between heavy-ions, for example, potential resonances emerge without being smeared out by the imaginary part. As the incident energy increases, the partial wave approaches the statistical yrast line or strong absorption region to the compound nucleus, while the next partial wave comes into the interaction region Of course a little absorption to the compound nucleus would exist even in the

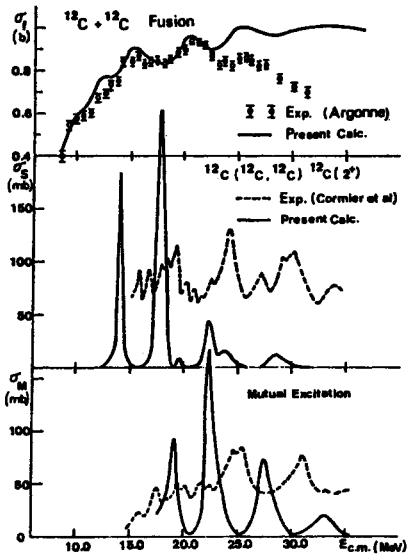

Fig. 21. Fragmentation of resonances in the inelastic channels of the $^{12}C+^{12}C$ system calculated by the present method, where the fragmentation mechanism and the fusion reaction are treated separately (see the text for details). The adopted values of the parameters are given in Table VII.

case where the level density is not so high and consequently some spreading of the resonance widths would be expected. Then one could expect a process where the formation of complicated compound nucleus states is achieved through molecular resonances as doorway states, as Feshbach[4] suggested. The prominent resonances in the ^{12}C-^{12}C system, however, do not seem to be such isolated doorway states as discussed above.

Finally we will briefly examine the consequence of our factorization of the absorption and resonance effects on the 90° elastic excitation function. Figure 22 shows the calculated results, together with the experimental data.[27] We see that the experimental intermediate structure is reproduced well by the BCM with a smooth-cutoff representation of absorption effects. Furthermore, we can recognize from the energy dependence of the elastic phase shifts, shown in the upper part of Fig. 22, that each calculated prominent peak corresponds approximately to a resonance obtained in the BCM with a real potential only. It is particularly striking that the characteristic doublet observed at $E_{c.m.} \simeq 20$ MeV is reproduced correctly by the present calculation as well as another small peak at a slightly lower energy. This is not haphazard but is a natural consequence of the BCM, because three bands, that is, the elastic and the aligned molecular bands, cross at about 20 MeV and $J^{\pi}=12^{+}$ as already illustrated in Fig. 6. In other words, these peaks may be considered as a reflection of the fragmentation of the 12^{+} elastic potential resonance strength.

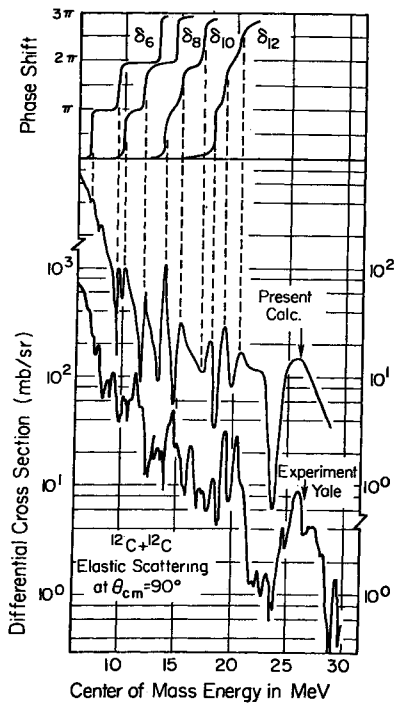

Fig. 22. Comparison of the results in the new treatment with the observed elastic exitation function at $\theta_{c.m.}=90°$ (Ref. 27)) in the $^{12}C+^{12}C$ system. Several phase shifts obtained in the BCM with real potential only are also shown in the upper part. In this calculation we include the coupling of single and mutual 2_1^{+} excitations and 3_1^{-} excitation of ^{12}C with the elastic channel. Adopted parameters are given in Table VII.

The fact that the calculated curve of Fig. 22 lacks structure corresponding to the experimental data at energies above $E_{c.m.} \cong 20$ Mev merely reflects the fact that in these calculations we have included only single and mutual excitations of the 2^+ state and 3^- state in ^{12}C. Data of Fulton et al.[26] show clearly that at higher energies the 4_1^+ member of the ^{12}C ground rotational band plays an important role, consistent with the band crossing diagram of Fig. 6.

It is worth remarking here that there is as yet no simple picture of the relation between the structure in the elastic excitation function and resonances, i.e., there is no simple general rule of the interference between the resonant and background amplitudes. The above analysis suggests that there is little interference in the $^{12}C+^{12}C$ system whereas the analysis in subsection 4.2. suggests destructive interference in the $^{16}O+^{16}O$ system. What we can infer concerning the reason for the different interference effects between the two systems is a difference in the absorption effects; the calculations show that in the latter system resonances in the entrance channel are rather smeared out and define resonance windows whereas in the former system some of the entrance channel resonances still persist.

§ 6. Discussion of resonances in other reaction channels

In the previous sections we have investigated resonances observed in the inelastic scattering, especially to collective excitations of the projectile and/or the target nucleus. Since the discovery of resonance phenomena in heavy-ion reactions,[2] experimental efforts have been made on various systems and in various reaction channels.[3] Particularly the ^{12}C-^{12}C system has been investigated extensively in α-, ^8Be- and nucleon-channels from sub-Coulomb energies to energies well above the Coulomb barrier. A large number of resonances have been observed around the grazing angular momentum as has been noted by several authors.[3] In the following we will mainly discuss these resonances.

The fact that many resonances have been found would appear to put in question the simple molecular picture proposed at the time of the disovery of the first resonances. As has been mentioned in § 1 the present authors[8] showed that a higher level density of resonant states could be reproduced by including up to the mutual excitation of the collective 2_1^+ (4.44 MeV) state, but this necessitated an arbitrary change of the potential depths in the inelastic channels. It still remains an interesting problem to investigate theoretically whether such interaction potentials are justified or not, as attempted by Park, Greiner and Scheid.[52] On the other hand it would be more reasonable to expect that other degrees of freedom may participate. Michaud and Vogt[7] proposed the picture of α-particle molecules, which Voit, Ischenko and Siller[53] supported by measuring large decay branching ratios of the excited sates of

^{20}Ne with α-clustering to the members of the ground rotational band. Thus it is hoped to develop a microscopic study of the many α-cluster system.[54]

Experimentally resonances in heavy-ion reactions have been observed fairly selectively not only in the incident channel but also in outgoing channels. This fact seems to demand a simple systematic explanation. The Florida group,[55] which has observed many resonances with the same spin in the ^{8}Be channel, and Feshbach[4] have proposed the picture of fragmentation of gross resonances; because of the gross structure resonances, windows exist for specific angular momentum at and within a few MeV of the resonance energy. These windows permit the carbon nuclei to be in close contact and to interact and thereby to fragment the gross resonances into a number of narrow doorway state resonances. Independently the present authors[8] have also done a fragmentation analysis and obtained the distribution of carbon partial widths among the 2^+ resonances near the Coulomb barrier.

Before proceeding to a discussion about the resonance mechanism, we will briefly review the analysis of the 2^+ resonances in the sub-Coulomb energy region of the ^{12}C-^{12}C system. We have used the Breit-Wigner formula for the resonant absorption cross section,

$$\sigma_J^R = \frac{2\pi}{k^2} \cdot (2J+1) \cdot \frac{\Gamma_\gamma \cdot \Gamma_c}{(E_{\text{c.m.}} - E_r)^2 + \Gamma^2/4} . \qquad (6\cdot1)$$

The total reaction width Γ_γ is assumed to be almost the same as the total width Γ, which is observed experimentally, and set to be 100 keV. From the experimental value of each peak height, we have obtained Γ_c for each resonance and then we have calculated the ratio $\Gamma_c/\Gamma_{\text{s.p.}}$, where $\Gamma_{\text{s.p.}}$ is the single particle width of the potential resonance calculated by a real potential with the depth adjusted to reproduce the observed resonance energy. Figure 23 shows the distribution of the strengths thus obtained. The error bars indicate ambiguities in extracting resonance contributions from the measured total reac-

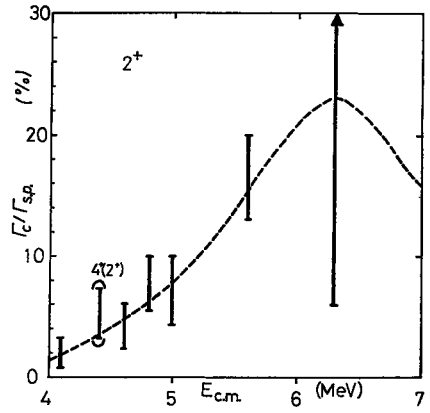

Fig. 23. Ratios $\Gamma_c/\Gamma_{\text{s.p.}}$ are shown for resonances with $J^\pi=2^+$, where Γ_c's are extracted from the experimental data (Ref. 56)). The dashed line is given for an eye-guide, which simply shows the strength distribution of fragmented potential resonances.

tion cross sections. We can clearly see the fragmentation of the 2^+ potential resonance among several intermediate resonances which have been observed in the total reaction cross sections[56] and in the total α-particle yields.[57] Recently the carbon partial width has been extracted from an analysis of the elastic scattering.[58] They have obtained a 2^+ resonance at $E_{c.m.}=6.6$ MeV with $\Gamma_c=29\pm6$ keV. This gives about 5% for the $\Gamma_c/\Gamma_{s.p.}$ by using $\Gamma_{s.p.}$ calculated in the same way as above. The dashed line drawn as an eye guide in Fig. 23 remains still correct semi-quantitatively. From Fig. 23, the original potential resonance with spin 2^+ is expected to exist at around 6 MeV in the C.M. energy. In the higher energy region fewer fragmented peaks have been observed. With the conjectured spins 12 and 14 at about $E_{c.m.}\cong20$ and 25 MeV, resonance strengths are concentrated mainly among a few inelastic channels. Thus we can guess approximate energies of the potential resonances with spins 12 and 14. Together with the position of the 2^+ resonance obtained in the above we now know approximately the position of the elastic molecular band in the ^{12}C-^{12}C system. This knowledge is very important in choosing the real part of the phenomenological interaction potential. An analysis such as the one described above, which extracts a partial width distribution, is necessary for all spin values to understand the resonance mechanism, for example, the fragmentation picture.

We now proceed to discuss a possible resonance mechanism as well as possible nuclear structures of resonance states, which gives rise to a fragmentation. The success of the BCM in the systematic explanation of the resonances observed in the inelastic channels urges us to apply it as a natural extention to resonances in other reaction channels. An important point in the BCM is that we can expect prominent resonance phenomena if energies of potential resonances in an entrance and exit channel are close to each other. If there is a series of potential resonances in some rearrangement channel, we can make a reliable prediction in the same way as before about the occurrence of resonances whose dominant components are molecular configurations of the entrance and exit channels. But usually there are ambiguities even in the real part of the interaction potential in rearrangement channels. Such ambiguities have already been encountered in the case of the inelastic channels which include the excitations of clustering states of the target or the projectile. Another difficulty is due to the difference between the effective moments of inertia of molecular bands of the entrance and exit channels. In the case of collective excitation discussed before we can safely assume the same moment of inertia for both channels. If there is a difference in the moment of inertia the band crossing region, where the two molecular bands are close to each other, is smaller. It is thus unfavorable for a systematic phenomenological analysis. We can, however, make qualitative arguments about such a possible region of resonances and about its relevance to observed resonances in various reaction

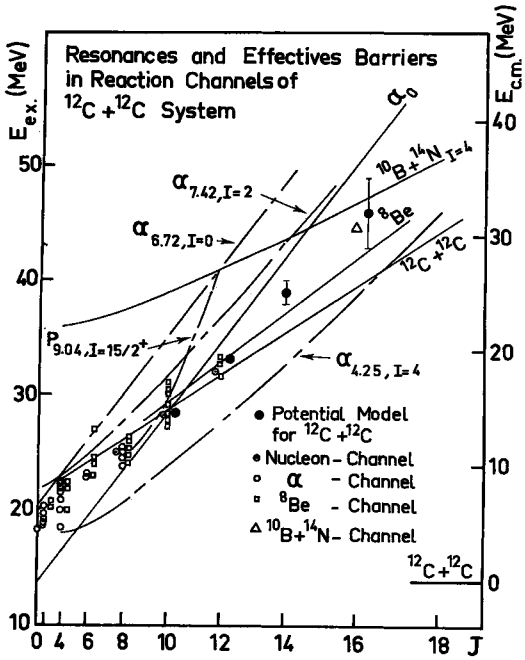

Fig. 24. Effective barriers in the aligned sub-channels of several reaction channels and resonances observed in the $^{12}C+^{12}C$ system. Data with symbol ⊙ are taken from Ref. 50) and those with symbols ○, □ and △ from Refs. 58), 60), Refs. 55), 61) and Ref. 59), respectively. Symbols ● indicate resonance energies calculated with the potential of Table I, which gives an approximate location of the molecular band in the $^{12}C+^{12}C$ system consistent with resonance data of Ref. 15).

channels, because the region for a potential resonance with observable width is rather limited around the top of the effective barrier in the channel considered.

In Fig. 24 the effective barrier heights in various reaction channels are shown together with the resonances observed in the compound nucleus ^{24}Mg. The molecular band in the ^{12}C-^{12}C elastic channel is also shown there, which has been evaluated by the present authors as explained in § 4.1. Resonances observed in the ^{12}C-^{12}C induced reactions should not be far away from the molecular band. At the same time resonances prominently observed in a specific exit channel, which would have two-body molecular configuration related to that channel as one of the dominant components, should be found around the effective barrier height as is stated above. First it is very interesting to note that the barrier height in the ^8Be channel is always close to the molecular band in the ^{12}C-^{12}C channel. We can thus expect that resonances will be observed prominently in this channel over a wide range of energies and spins, which corresponds to the recent observation by Florida group.[55] The ^8Be-^{16}O* configurations will also play an important role at higher energies and spins. As for the α-channels, α-^{20}Ne* configurations, for some of which the barrier heights are shown in Fig. 24, will also play a dominant role at lower spins, whereas members of the ground rotational band of ^{20}Ne will take part at spins higher than about 8. Thus the enhanced decays to some excited states of ^{20}Ne observed by Voit et al.[53] are consistent with our picture, without assuming α-particle molecular configurations. Several resonances observed in

proton channels[50] might suggest the existence of compound states with special nuclear structures. We again can expect that they have two-body configurations of p-^{23}Na* as dominant components, because the barrier heights of the relevant channels are fairly close to the resonances and to the molecular band in the ^{12}C-^{12}C channel at their conjectured spin values. Finally the resonances recently observed in the ^{10}B-^{14}N exit channels[59] also seem to be consistent with the present picture. From the effective barrier heights shown in Fig. 24, we can expect rather sharp resonances with a two-body ^{10}B+^{14}N molecular configuration, sharper than those in the ^{12}C-^{12}C configurations at spins 16^+ and 18^+ etc, which will couple strongly with the ^{12}C-^{12}C elastic and inelastic molecular configurations.

All the characteristic features of resonances observed in various reaction channels seem to be consistent with the BCM, although we have not yet made a quantitative study of them. This is mainly due to the lack of knowledge of the interactions between heavy-ions in the exit channels. Of course we can proceed further by assuming plausible interactions. Such attempts have already been made by the present authors[14g),25] and the results are encouraging. What is now required in the experimental study is the measurement of essential data, such as excitation functions of elastic scattering in various combinations of heavy-ions, angle-integrated excitation function of various reaction processes and so on. These would allow us to extract the distributions of various partial widths among resonances. This is of course applicable to other heavy-ion systems such as ^{12}C-^{16}O and ^{16}O-^{16}O.

§ 7. Summary

The existence or non-existence of a molecular configuration in a nucleus has been an interesting question since resonances were first discovered in heavy-ion reactions. Measurements of the elastic scattering excitation functions at high energies and subsequent optical model analyses have shown the existence of surface transparency in the interactions between several combinations of heavy-ions.[10] The observed intermediate structure might suggest that there exists a wide energy region of resonances with molecular configurations. On the other hand it has been shown possible to encompass all the observed structure within the framework of a purely statistical model.[64] Of course this does not imply that the observed data have necessarily a statistical origin, but means that in order to claim the molecular origin for structure in such excitation functions it is necessary to uncover more detailed signatures for it or to correlate specific structural details of the data with detailed predictions of molecular models.

The present authors[12] have proposed the BCM as a mechanism for occurrence of resonances with two-body nuclear molecular configurations. As is explained in § 2 the model is a natural simplification and development of Nogami-Imanishi model and allows us to predict where and with what spin

values resonances will appear with specific molecular configurations. Consequently it provides predictions concerning the nuclear structures of resonances; first, the aligned configurations of a channel spin and an orbital angular momentum will dominate in prominent resonances, and second, a systematic change of the nuclear structure among resonances will take place depending on the intrinsic spin and the excitation energy of the target and/or the projectile nucleus as is readily seen from the differences in the crossing points. The former prediction could be checked by polarization-type measurements. The latter one has already been confirmed partly by several experiments.[16d),26)]

It is fortunate as is shown in § 5 that the predicted energy region for molecular resonances just overlaps with that of surface transparency whose existence has been recognized for a long time and whose origin has been clarified recently in connection with our understanding of heavy-ion fusion reactions. Quantitative investigations on the region of surface transparency are now in progress for confirmation.[45)]

In § 4 the results of the coupled-channel calculations based on the BCM have been summarized. The comparisons with available experimental data lead us to the conclusion that the BCM can systematically reproduce characteristic features, i.e., energies, widths and yields of resonances observed in the elastic and inelastic scattering of the ^{12}C-^{12}C, ^{12}C-^{16}O and ^{16}O-^{16}O systems, over a wide energy region. Although we have not yet understood the structures of resonances with low spins including the three resonances discovered at Chalk River, we are now confident that two-body nuclear molecular configurations with various intrinsic excitations exist in these systems, i.e., among highly excited states with high spins in ^{24}Mg, ^{28}Si and ^{32}S. The existence of such a region, i.e., "molecular resonance region" can be expected in other systems satisfying the same condition as is discussed in § 5. Recently Haas[36)] has shown that almost all the combinations of Carbon and Oxygen isotopes have resonance structures in inelastic and transfer channels. They are likely to have a "molecular resonance region".

It seems to be interesting and promising to extend the BCM calculations to various systems with the inclusion of excitations of clustering states and of rearrangement channels as is surmised also from the discussion in § 6. Another interesting subject is to study the origin of the imaginary part of the interaction potential between heavy-ions along the direction given in § 5, which will lead us to a comprehensive understanding of the reaction mechanism and hence of the interaction between light heavy-ions.

Acknowledgements

The authors would like to express their thanks to Professor K. Ikeda and Professor R. Tamagaki for their encouragements and discussions in

the course of the studies, the results of which are summarized in the present chapter. Most of the studies have been performed mainly as part of the annual project on "Highly Excited States in Nuclei and Molecular Resonances" organized by the Research Institute for Fundamental Physics, Kyoto University since 1976. The authors thank all the members of the project.

They also appreciate the encouragement by Professor A. Arima, Professor D. A. Bromley and Professor S. M. Lee who have kindly permitted them to include some recent results obtained by collaboration. One of the authors (Y. A.) appreciates encouragements given by Professor H. Tanaka and acknowleges the financial support by "Institut de Physique Nucléaire et de Physique des Particules" and is grateful for the kind hospitalties extended to him by Professor A. Gallmann, Dr. J. P. Coffin, Dr. F. Haas, Dr. R. M. Freeman and other members of Centre de Recherches Nucléaires, Strasbourg during his stay, while most of the manuscript was prepared. Activities of one of the authors (Y. K.) has been partly supported by the National Science Foundation. The authors gratefully acknowledge the comments given by Dr. R. M. Freeman and Dr. C. M. Vincent, and their careful readings of the manuscript. They also thank Miss D. Kueny for typing the manuscript.

References

1) a) K. Ikeda, N. Takigawa and H. Horiuchi, Prog. Theor. Phys. Suppl. Extra Number (1969), 464.
b) H. Horiuchi, K. Ikeda and Y. Suzuki, Prog. Theor. Phys. Suppl. No. 52 (1972), 89.
c) A. Tohsaki, F. Tanabe and R. Tamagaki, Prog. Theor. Phys. **45** (1971), 980.
2) E. Almqvist, D. A. Bromley and J. A. Kuehner, Phys. Rev. Letters **4** (1960), 515.
3) a) R. H. Siemssen, *Proc. INS-IPCR Symp. on Cluster Structure of Nuclei and Transfer Reactions Induced by Heavy-Ions*, edited by H. Kamitsubo, I. Kohno and T. Marumori (Tokyo, 1975), p. 233.
b) D. A. Bromley, *Proc. Second Intern. Conf. on Clustering Phenomena in Nuclei*, edited by D. Goldman, J. B. Marion and S. J. Wallace (Maryland, 1975), p. 465.
c) D. A. Bromley, *Nuclear Molecular Phenomena*, edited by N. Cindro (North-Holland Amsterdam, 1978), p. 3.
d) P. Taras, *Proc. Third Intern. Conf. on Clustering Aspects of Nuclear Structure and Nuclear Reactions*, edited by W. T. H. Van Oers, J. P. Svenne, J. S. C. McKee and W. R. Falk (Winnipeg, 1978), p. 234.
e) F. Haas, *Proc. Colloque Franco-Japonais* (Paris, 1979).
R. M. Freeman, F. Haas and G. Korschinek, Phys. Letters **90B** (1980), 229.
R. M. Freeman, *Proc. Intern. Conf. on Resonant Behavior of Heavy-Ion Systems* (Athens, 1980).
4) H. Feshbach, J. de Phys. Colloq. **37** (1976), C5-177.
5) M. Nogami, private communication.
6) B. Imanishi, Nucl. Phys. **A125** (1969), 33.
7) G. J. Michaud and E. W. Vogt, Phys. Rev. **C5** (1972), 350.
8) Y. Kondō, T. Matsuse and Y. Abe, Prog. Theor. Phys. **59** (1978), 465.
9) W. Scheid, W. Greiner and R. Lemmar, Phys. Rev. Letters **25** (1970), 176.
10) a) A. Gobbi, R. Wieland, L. Chua, D. Shapira and D. A. Bromley, Phys. Rev. **C7** (1973), 30.
b) R. A. Chatwin, J. S. Eck, D. Robson and A. Richter, Phys. Rev. **C1** (1970), 795.

c) R. H. Siemssen, *Nuclear Molecular Phenomena*, edited by N. Cindro (North-Holland, Amsterdam, 1978), p. 79.
11) a) S. M. Lee, T. Matsuse and A. Arima, Phys. Rev. Letters **45** (1980), 165.
A. Arima, T. Matsuse and S. M. Lee, *Proc. Colloque Franco-Japonais* (Paris, 1979). See also
b) R. Vandenbosch, Phys. Letters **87B** (1979), 183.
12) a) T. Ando, K. Ikeda and Y. Suzuki, Prog. Theor. Phys. **54** (1975), 119.
b) T. Ando, K. Ikeda and A. Tohsaki-Suzuki, Prog. Theor. Phys. **61** (1979), 101.
13) D. Baye and P.-H. Heenen, Nucl. Phys. **A283** (1977), 176.
14) a) Y. Kondō, T. Matsuse and Y. Abe, *Proc. INS IPCR Symp. on Cluster Structure of Nuclei and Transfer Reactions Induced by Heavy-Ions*, edited by H. Kamitsubo et al. (Tokyo, 1975), p. 280.
b) Y. Abe, *Proc. Second Intern. Conf. on Clustering Phenomena in Nuclei*, edited by D. Goldman et al. (Maryland, 1975), p. 500.
c) T. Matsuse, Y. Kondō and Y. Abe, Prog. Theor. Phys. **59** (1978), 1009.
d) T. Matsuse, Y. Abe and Y. Kondō, Prog. Theor. Phys. **59** (1978), 1037.
e) Y. Abe, Y. Kondō and T. Matsuse, Prog. Theor. Phys. **59** (1978), 1393.
f) T. Matsuse, Y. Abe and Y. Kondō, Prog. Theor. Phys. **59** (1978), 1904.
g) Y. Abe, *Nuclear Molecular Phenomena*, edited by N. Cindro (North-Holland, Amsterdam, 1978), p. 211.
h) Y. Abe, *Proc. Third Intern. Conf. on Clustering Aspects of Nuclear Structure and Nuclear Reactions*, edited by W. T. H. Van Oers et al. (Winnipeg, 1978), p. 132.
i) Y. Kondō, Y. Abe and T. Matsuse, Phys. Rev. **C19** (1979), 1356.
j) Y. Kondō and D. A. Bromley, Bull. Am. Phys. Soc. **24** (1979), 556.
Y. Kondō, D. A. Bromley and Y. Abe, Prog. Theor. Phys. **63** (1980), 722; Phys. Rev. **C22** (1980), 1068.
15) a) T. M. Cormier, J. Applegate, G. M, Berkowitz, P. M. Cormier, J. W. Harris, C. M. Jachcinski, L. L. Lee, Jr., J. Barrette and H. E. Wegner, Phys. Rev. Letters **38** (1977), 940.
b) T. M. Cormier, C. M. Jachcinski, G. M. Berkowitz, P. Braun-Munzinger, P. M. Cormier, M. Gai, J. W. Harris, J. Barrette and H. E. Wegner, Phys. Rev. Letters **40** (1978), 924.
16) a) R. E. Malmin, R. H. Siemssen, D. A. Sink and P. P. Singh, Phys. Rev. Letters **28** (1972), 1590.
See also R. Stockstad, D. Shapira, L. Chua, P. Parker, M. W. Sachs, K. Wieland and D. A. Bromley, Phys. Rev. Letters **28** (1972), 1523.
b) C. M. Jachcinski, T. M. Cormier, P. Braun-Munzinger, G. M. Berkowitz, P. M. Cormier, M. Gai and J. W. Harris, Phys. Rev. **C17** (1978), 1263.
c) D. Shapira, R. M. DeVries, M. R. Clover, R. N. Boyd and R. N. Cherry, Jr., Phys. Letters **71B** (1977), 293.
d) K. Katori, K. Furuno and T. Ooi, Phys. Rev. Letters **40** (1978), 1489.
K. Furuno, K. Katori, T. Aoki, T. Ooi and J. Sanada, Nucl. Phys. **A321** (1979), 250.
e) R. E. Malmin, J. W. Harris and P. Paul, Phys. Rev. **C18** (1978), 163.
f) D. Branford, B. N. Nagorcka and J. O. Newton, J. of Phys. **G3** (1977), 1565.
g) C. M. Jachcinski, P. Braun-Munzinger, G. M. Berkowitz, R. H. Freifelder, M. Gai, R. L. McGrath, P. Paul, J. Renner and C. D. Uhlhorn, Phys. Letters **87B** (1979), 354.
h) J. R. Beene, D. Shapira, R. M. DeVries and M. R. Clover, Phys. Rev. **C21** (1980), 167.
17) J. J. Kolata, R. M. Freeman, F. Haas, B. Heusch and A. Gallmann, Phys. Rev. **C19** (1979), 2237.
18) P. L. Phillips, K. A. Erb, D. A. Bromley and J. Weneser, Phys. Rev. Letters **42** (1979), 566.
19) a) I. Shimodaya, R. Tamagaki and H. Tanaka, Prog. Theor. Phys. **27** (1962), 793.
b) A. Tohsaki, F. Tanabe and R. Tamagaki, Prog. Theor. Phys. **53** (1975), 1022.
20) a) R. Satchler and W. G. Love, Phys. Reports **C55** (1979), 183.
b) O. Tanimura, Nucl. Phys. **A309** (1978), 233.
c) O. Tanimura and T. Tazawa, Phys. Letters **83B** (1979), 22; Phys. Rev. **C20** (1979), 183.

21) T. Tamura, Rev. Mod. Phys. **37** (1965), 679.
22) W. Kohn, Phys. Rev. **74** (1948), 1763.
L. Hulthén, Ark. Mat., Astr. Fys. **35A** (1948), n° 25.
23) Y. Mito and M. Kamimura, Prog. Theor. Phys. **56** (1976), 583.
M. Kamimura, Prog. Theor. Phys. Suppl. No. 62 (1977), 236.
24) N. F. Mott and H. S. W. Massey, *The Theory of Atomic Collisions* (Oxford Univ. Press, 1965, the third edition), Chaps. VI and XIII.
25) T. Matsuse, *Nuclear Molecular Phenomena*, edited by N. Cindro (North-Holland, Amsterdam, 1978), p. 247.
26) B. R. Fulton, T. M. Cormier and B. J. Herman, Phys. Rev. **C21** (1980), 198.
27) W. Reilly, R. Wieland, A. Gobbi, M. W. Sachs, J. Maher, R. H. Siemssen, D. Mingay and D. A. Bromley, Nuovo Cim. **13A** (1973), 913.
28) P. P. Singh, D. A. Sink, P. Schwandt, R. E. Malmin and R. H. Siemssen, Phys. Rev. Letters **28** (1972), 1714.
29) J. V. Maher, M. W. Sachs, R. H. Siemssen, A. Weidinger and D. A. Bromley, Phys. Rev. **188** (1969), 1665.
30) a) B. Fernandez, C. Gaarde, J. S. Larsen, S. Pontoppidan and F. Videbaek, Nucl. Phys. **A306** (1978), 259.
b) I. Tserruya, Y. Eisen, D. Pelte, A. Gavron, H. Oeschler, D. Berndt and H. L. Harney, Phys. Rev. **C18** (1978), 1688.
c) V. K. C. Cheng, A. Little, H. C. Yuen, S. M. Lazarus and S. S. Hanna, Nucl. Phys. **A322** (1979), 168.
d) F. Saint-Laurent, M. Conjeaud, S. Harar, J. M. Loiseaux, J. Menet and J. B. Viano, Nucl. Phys. **A327** (1979), 517.
e) D. G. Kovar, D. F. Geesaman, T. H. Braid, Y. Eisen, W. Henning, T. R. Ophel, M. Paul, K. E. Rehm, S. J. Sanders, P. Sperr, J. P. Schiffer, S. L. Tabor, S. Vigdor, B. Zeidman and F. W. Prosser, Jr., Phys. Rev. **C20** (1979), 1305. And see also Ref. 17).
31) J. J. Kolata, R. C. Fuller, R. M. Freeman, F. Haas, B. Heusch and A. Gallmann, Phys. Rev. **C16** (1977), 891.
32) D. L. Hanson, R. G. Stokstad, K. A. Erb, C. Olmer, M. W. Sachs and D. A. Bromley, Phys. Rev. **C9** (1974), 1760.
33) J. P. Schiffer, *Proc. Intern. Conf. on Nuclear Phys. Münich, Vol. 1* (1973), p. 813.
34) P. Charles, F. Auger, I. Badawy, B. Berthier, M. Dost, J. Gastebois, B. Fernandez, S. M. Lee and E. Plagnol, Phys. Letters **62B** (1976), 289.
35) R. L. Malmin and P. Paul, *Proc. Second Intern. Conf. on Clustering Phenomena in Nuclei*, edited by D. Goldman et al. (Maryland, 1975), p. 540.
And see also Ref. 16e).
36) H. G. Bohlen, W. Bohne, B. Gebauer, W. von Oertzen, M. Goldschmidt, H. Hafner, L. Pflug and K. Wannebo, Phys. Rev. Letters **37** (1976), 195.
S. J. Willett et al., to be published.
37) D. G. Kovar, *IPCR Cyclotron Progress Report Supplement* **6** (1977), p. 18.
And see also Ref. 30e).
38) a) J. Galin, D. Guerreau, M. Lefort and X. Tarrago, Phys. Rev. **C9** (1974), 1018.
b) M. Lefort and C. Ngo, Ann. de Phys. **3** (1978), 5.
39) D. Glas and U. Mosel, Nucl. Phys. **A237** (1975), 429.
40) M. Lefort, J. de Phys. Colloq. **33** (1976), C5-73.
41) D. Glas and U. Mosel, Phys. Letters **78B** (1978), 9.
42) a) J. P. Schiffer, *Proc. of Colloque Franco-Japonais de Spectroscopie Nucléaire et Réaction Nucléaire* (Dogashima, 1976), p. 176.
b) R. G. Stokstad, *Proc. of Topical Conference on Heavy-Ion Collisions* (Tennessee, 1977), p. 22.
43) C. Mahaux and H. A. Weidenmüller, *Shell-Model Approach to Nuclear Reactions* (North-Holland, Amsterdam, London, 1969).

44) A. Tohsaki-Suzuki, Prog. Theor. Phys. Suppl. No. 62 (1977), 197; Soryushiron Kenkyu (Kyoto) **54** (1976), B47.
45) F. Haas and Y. Abe, in preprint.
Y. Abe, *Proc. Intern. Conf. on Resonant Behavior of Heavy-Ion Systems* (Athens, 1980).
46) Y. Abe, T. Matsuse and Y. Kondō, Phys. Rev. **C19** (1979), 1365.
47) W. E. Frahn and R. H. Venter, Ann. of Phys. **24** (1963), 243.
48) K. W. Ford, D. L. Hill, M. Wakano and J. A. Wheeler, Ann. of Phys. **7** (1959), 239.
49) P. Sperr, T. H. Braid, Y. Eisen, D. G. Kovar, F. W. Prosser, Jr., J. P. Schiffer, S. L. Tabor and S. E. Vigdor, Phys. Rev. Leters **37** (1976), 321.
50) E. R. Cosman, T. M. Cormier, K. Van Bibber, A. Sperduto, G. Young, J. Erskine, L. R. Greenwood and O. Hansen, Phys. Rev. Letters **35** (1975), 265.
51) J. J. Kolata, R. M. Freeman, F. Haas, B. Heusch and A. Gallmann, Phys. Rev. **C19** (1979) 408.
52) J. Y. Park, W. Greiner and W. Scheid, Phys. Rev. **C16** (1977), 2276.
53) H. Voit, G. Ischenco and F. Siller, Phys. Rev. Letters **30** (1973), 564.
54) A. Tohsaki-Suzuki, Prog. Theor. Phys. **60** (1978), 1013.
55) a) N. R. Fletcher, J. D. Fox, G. J. Kekelis, G. R. Morgan and G. A. Norton, Phys. Rev. **C13** (1976), 1173.
b) D. R. James and N. R. Fletcher, Phys. Rev. **C17** (1978), 2248.
56) M. Spinka and H. Winkler, Nucl. Phys. **A233** (1974), 456.
57) H. Voit, W. Galster, W. Treu, H. Fröhlich and P. Dück, Phys. Letters **67B** (1977), 399.
58) S. K. Korotky, K. A. Erb, S. J. Willett and D. A. Bromley, Phys. Rev. **C20** (1979), 1014.
59) M. R. Clover, T. M. Cormier, B. R. Fulton and B. J. Herman, Phys. Rev. Letters **43** (1979), 256.
60) W. Galster, W. Treu, P. Dück, H. Fröhlich and H. Voit, Phys. Rev. **C15** (1977), 950.
61) R. Wada, J. Schimizu and K. Takimoto, Phys. Rev. Letters **38** (1977), 1341.
62) M. Conjeaud, S. Gary, S. Harar and J. P. Wieleczko, Nucl. Phys. **A309** (1978), 515.
63) D. Horn and A. J. Ferguson, Phys. Rev. Letters **41** (1978), 1529.
64) D. Shapira, R. G. Stokstad and D. A. Bromley, Phys. Rev. **C10** (1974), 1063.